Engineered Science
DOI: https://dx.doi.org/10.30919/es1828

A Short Review of Density Functional Theory Studies into Hydrogen Storage in Metal-Organic Frameworks

Raushan Soltan,[1,2,5] Ayaulym Amankeldiyeva,[1] Beksultan Akilbekov,[1] Madina Kalibek,[1] Saniya Sarsenova,[3] Zhambul Kerimkulov,[4] Munziya Abutalip,[1,5] Yerbolat Magazov,[1] Nurlan Almas,[1] Nurxat Nuraje[1,5,6,*] and Mirat Karibayev[1,5*]

Abstract

This review critically examines recent Density Functional Theory (DFT) studies on hydrogen storage in Metal-Organic Frameworks (MOFs). We focus on how DFT provides fundamental insights into the electronic-level interactions governing hydrogen uptake. The analysis reveals that MOFs can be rationally designed for enhanced hydrogen storage capacity by tuning their structural and electronic properties. DFT has found several key techniques, including changing pore size and linker chemistry, substituting or functionalizing frameworks with light metals such as Li and Sc, and introducing open metal sites. The article discusses how DFT simulations accurately anticipated optimal binding energies for H_2 physisorption and highlighted the importance of backdonation from metal d-orbitals to hydrogen σ^* orbitals in strengthening interactions. Furthermore, we show that DFT-guided material design results in anticipated capacities that meet or surpass DOE requirements for onboard hydrogen storage. This work underscores the indispensable role of DFT as a predictive tool, enabling the efficient screening and development of MOF materials with superior performance for the future hydrogen economy.

Keywords: Density functional theory; Metal-organic frameworks; Hydrogen storage; Physisorption; Material design.
Received: 15 August 2025; Revised: 16 October 2025; Accepted: 21 October 2025
Article type: Review article.

1. Introduction

1.1 Hydrogen storage needs for the hydrogen economy

Hydrogen has emerged as one of the most promising clean energy carriers for enabling a sustainable, low-carbon energy economy. Its high gravimetric energy density (120 MJ/kg) significantly exceeds that of conventional fossil fuels, and when used in fuel cells or combustion, hydrogen produces only water as the by-product, avoiding greenhouse gas emissions.[1-3] These attributes make hydrogen a central element in future energy transition scenarios, supporting applications ranging from stationary power generation to fuel-cell electric vehicles (FCEVs) and portable electronics. Furthermore, in a hydrogen fuel cell operation, hydrogen oxidation yields just water vapor, avoiding carbon dioxide and other hazardous emissions associated with fossil fuel combustion. This combination of great energy efficiency and zero greenhouse gas emissions establishes hydrogen as a superior and sustainable energy carrier for a low-carbon future.[4] However, the practical implementation of a hydrogen economy is critically constrained by the challenge of safe, efficient, and cost-effective hydrogen storage.

Unlike liquid hydrocarbons, hydrogen exists as a light diatomic gas under ambient conditions, with a low volumetric density of only 0.089 g/L at 298 K and 1 bar. The challenge occurs because hydrogen, as the smallest and lightest molecule, is particularly difficult to confine efficiently. Because of its low volumetric density and high diffusivity, storing enough hydrogen for practical application necessitates the employment of high pressures, cryogenic temperatures, or sophisticated solid-state materials, all of which present safety, cost, and reversibility trade-offs.[5] Each approach carries inherent limitations.[6-10] High-pressure gaseous storage (typically 350–700 bar) requires robust containment systems that are heavy, energy-intensive, and costly to manufacture. Cryogenic liquid storage at 20 K offers high volumetric densities but suffers from boil-off losses, high energy input for

[1]*Laboratory of Renewable Energy, National Laboratory Astana, Nazarbayev University, 53 Kabanbay Batyr avenue, Astana, 010000, Kazakhstan*
[2]*Laboratory of Engineering Profile, Satbayev University, 22a, Satbayev Street, Almaty, 050013, Kazakhstan*
[3]*Astana International University, 8 Kabanbay Batyr avenue, Astana, 020000, Kazakhstan*
[4]*Abay Myrzakhmetov Kokshetau University, Kokshetau, 020000, Kazakhstan*

liquefaction, and long-term safety concerns. These limitations have motivated intense research into materials-based storage technologies, where hydrogen can be reversibly adsorbed or absorbed into engineered solids. As a result, building a storage system that is lightweight, compact, safe, and economical remains one of the most persistent hurdles to achieving the hydrogen economy.

The U.S. Department of Energy (DOE) and other international agencies have set ambitious system-level targets for hydrogen storage. These include high gravimetric (≥5.5 wt%, in earlier plans) and volumetric (≥40 g H_2/L, in earlier plans) capacities, fast uptake and release kinetics, ambient operating conditions, long cycle life, and low cost.[6-11] Achieving such performance in a single storage system remains a formidable challenge, stimulating worldwide efforts to develop advanced adsorbent materials such as metal hydrides, complex hydrides, porous carbons, and framework materials. Metal-organic frameworks (MOFs) have received a lot of attention as a hydrogen storage material due to their hybrid organic-inorganic structures. This structural adaptability enables fine control over pore size, shape, and functionality, allowing for the optimization of hydrogen adsorption sites. MOFs' extraordinarily high surface area increases storage capacity, while their variable porosity and functionalization potential allow for the control of binding strength and adsorption kinetics. As a result, MOFs stand out as a promising platform for attaining reversible, high-density hydrogen storage that is consistent with DOE system-level goals.

For vehicular applications, hydrogen storage systems must provide a driving range comparable to gasoline vehicles while maintaining safety and efficiency. This requires not only high storage capacity but also rapid refueling times, thermal management, and compatibility with onboard fuel cell systems. In stationary applications, long-term stability and low operating costs are equally crucial. Thus, hydrogen storage research must simultaneously address multiple, sometimes conflicting requirements.

In this context, atomistic modeling and simulation play a vital role by revealing the fundamental interactions that govern hydrogen uptake, diffusion, and release in candidate materials. Insights from DFT calculations guide rational design strategies for tailoring framework structures toward meeting DOE targets. Therefore, a systematic understanding of hydrogen storage challenges is essential as the foundation for evaluating the role of MOFs in the hydrogen economy.

1.2 Why MOFs are attractive (tunable pores, high surface area, functionalization potential)

MOFs are a unique class of crystalline porous materials assembled from metal-containing clusters or ions connected by organic linkers. This hybrid composition allows unprecedented structural and chemical diversity, making MOFs highly attractive candidates for hydrogen storage applications.[7-12] Compared to traditional porous adsorbents such as activated carbons or zeolites, MOFs offer far greater tunability in pore architecture, chemical functionality, and framework stability, enabling the rational design of materials that approach the ambitious performance targets set for hydrogen storage in the hydrogen economy.

One of the defining features of MOFs is their extraordinarily high surface area. Many MOFs exhibit Brunauer–Emmett–Teller (BET) surface areas exceeding 5,000 m²/g, with pore volumes that can surpass those of any other known porous material. This immense internal surface area provides abundant adsorption sites for hydrogen molecules, directly correlating with high gravimetric and volumetric storage capacities. For example, benchmark MOFs such as MOF-5 and HKUST-1 have demonstrated impressive hydrogen uptake capacities under cryogenic conditions, underscoring the potential of MOFs as next-generation storage media.[8-13]

Equally important is the tunability of MOF pore structures. By carefully selecting the organic linkers and metal nodes, researchers can synthesize frameworks with a wide range of pore sizes, geometries, and topologies. This tunability allows optimization of pore environments for hydrogen adsorption, ensuring that interactions are neither too weak to retain hydrogen nor too strong to hinder release. The pore size of MOFs plays a crucial role in governing hydrogen adsorption behavior. Pores within the 0.7–1.2 nm range are considered optimal, as they are large enough to accommodate hydrogen molecules while narrow enough to enhance van der Waals interactions between the gas and the pore walls.[9-14] This balance maximizes physisorption capacity without impeding molecular diffusion or hydrogen release, making fine pore tuning an essential strategy in the design of high-performance MOF-based hydrogen storage materials.

Beyond structural design, MOFs offer tremendous potential for chemical functionalization. Introducing open metal sites, unsaturated coordination positions, or specific functional groups into the framework enhances the interaction energy between hydrogen molecules and the host material. For instance, doping with light metals such as Li, Mg, or Ca can increase the binding enthalpy to values closer to the ideal range (15–20 kJ/mol), facilitating hydrogen storage at near-ambient temperatures.[10-15] Similarly, post-synthetic modification allows the incorporation of electron-rich groups, catalytic moieties, or polar sites that strengthen hydrogen adsorption and improve selectivity.

Another compelling advantage of MOFs lies in their modular synthesis. Thousands of distinct MOF structures have already been reported, and high-throughput computational

[5]*Teqnovate LLC, Astana, 010000, Kazakhstan*
[6]*Department of Chemical and Materials Engineering, School of Engineering and Digital Sciences, Nazarbayev University, 53 Kabanbay Batyr Avenue, Astana, 010000, Kazakhstan*
[*]*Email:* nurxat.nuraje@nu.edu.kz (Nurxat Nuraje), mirat.karibayev@nu.edu.kz (Mirat Karibayev)

screening combined with atomistic simulations continues to expand the discovery space.[12-20] This versatility means that MOFs can be purpose-designed to meet specific performance metrics, whether for mobile storage in fuel-cell vehicles or for large-scale stationary energy storage.

MOFs' hybrid organic-inorganic composition allows for greater flexibility in processing and integration. MOFs may be inserted into composites, pellets, or membranes without significantly reducing porosity, which is critical for converting laboratory results into practical devices. MOFs are among the most promising materials for solving the fundamental problems of hydrogen storage in a clean energy economy due to their large surface areas, adjustable porosity, and functionalization possibilities.

1.3 MOFs nomenclature

MOFs have swiftly emerged as a popular class of porous crystalline materials due to their variable composition and structural variety. These compounds are often formed by connecting metal ions or clusters to multidentate organic ligands, resulting in extended frameworks with persistent porosity. In the literature, such systems have been referred to by various names, including hybrid organic-inorganic materials, metal-organic polymers, coordination polymers, and organic zeolite analogues. Among these, the term MOF has become the most extensively used, stressing both their inorganic-organic hybrid origin and their strong three-dimensional architecture.[21-25]

The abbreviation MOF is widely used as a generic designation for the entire class of materials. When preceded by a numeral, such as MOF-5 or MOF-177, it refers to a specific framework inside the class. This number naming standard has resulted in a clear and identifiable system that allows academics to differentiate between different structures and trace the progress of increasingly complicated frameworks. Members of the isoreticular MOF (IRMOF) series, such as IRMOF-1 and IRMOF-8, have the same topology but varied in pore size and functionality, demonstrating how systematic expansion within a family can result in frameworks with tunable properties.[26–30]

Many MOFs are identified not only by their numerical names, but also by the institutions or research organizations where they were first synthesized. Common examples include UiO (University of Oslo), MIL (Institut Lavoisier Materials), HKUST (Hong Kong University of Science and Technology), and LIC (Lanzhou Institute of Chemical Physics). Such terms have grown common in the field, frequently denoting families of frameworks with related synthetic techniques or topological properties.[31-34]

Table 1 provides an overview of the major Metal–Organic Frameworks (MOFs) reviewed in this work, highlighting their structural features, composition, and functional characteristics. Each MOF is described based on its metal node, organic linker, and pore architecture, which

Table 1: List of MOFs reviewed in this work with their general description.

Names	Description
IRMOF-1	$Zn_4O(BDC)_3$ framework with large cubic pores and high surface area.
IRMOF-10	Expanded IRMOF with longer linkers (BDC derivative), offering larger pore volume.
IRMOF-16	Highly porous Zn-based framework with extended linkers enhancing surface area and tunable pore size.
MOF-5	$Zn_4O(BDC)_3$ cubic network; archetype MOF with exceptional crystallinity.
MOF-74	Open metal sites (*e.g.*, Mg, Ni, Co) with helical channels and strong gas–framework interactions.
MOF-199	$Cu_3(BTC)_2$ framework with open Cu(II) sites and high adsorption capacity.
205	Zn-based MOF with hierarchical microporous–mesoporous structure and high connectivity.
MOF-525	Zirconium-based porphyrinic framework (Zr_6 nodes linked by TCPP ligands).
MOF-650	Zn-based large-pore MOF with aromatic linkers providing extended π–π stacking.
MOF-801	Zirconium–fumarate framework with robust structure and hydrophilic pores.
Triphenylene-hexathiol-based MOF	Conductive 2D π–π stacked framework formed via sulfur coordination.
Mn(II)-based MOF $[(Mn_4Cl)_3(BTT)_8]_8$	Magnetic MOF with Mn clusters linked by BTT ligands forming 3D cages.
M_2Cl_x(btdd) MOFs	Microporous frameworks with open metal sites and btdd ligands.
Prototypical MOFs, $Zn_4O(BDC)_3$ and $Cu_3(BTC)_2$	Benchmark MOFs with high stability and tunable pore environments.

Names	Description
Heterofullerene-linked MOF, $C_{48}B_{12}$-MOF	Framework connected by boron-doped fullerene linkers enhancing electronic conductivity.
Hafnium–melamine metal-organic framework (Hf-MEL MOF)	Hf_6 clusters coordinated with melamine-derived ligands forming stable 3D networks.
M(BDC)(TED)0.5 metal organic framework	Pillared-layered MOF formed by metal–BDC layers connected via TED linkers.
Sodalite-Type Metal–Organic Framework	3D cubic topology resembling zeolitic sodalite with small pore windows.
Borazocine-based metal–BN frameworks (MBFs)	Metal–boron–nitrogen frameworks with borazocine ligands offering thermal stability.
MFM-300(In)	Indium-based MOF with μ_2-OH bridges and flexible channels.

govern its adsorption and catalytic behavior. The table also summarizes their primary applications, including hydrogen storage, gas separation, catalysis, and environmental remediation.

1.4 Scope of review: atomistic-level insights

The current review focuses solely on the impact of DFT in enhancing our understanding of hydrogen storage in metal-organic frameworks. While other computational approaches, such as classical molecular dynamics or grand canonical Monte Carlo simulations, have yielded useful results, our focus here is on first-principles computations. DFT provides a powerful quantum-mechanical framework for investigating the fundamental characteristics of hydrogen interaction with MOFs, allowing predictions that exceed empirical findings and force-field-based approaches.

One of the primary benefits of DFT in hydrogen storage investigations is its ability to capture the electrical structure of MOFs with atomic precision. It enables direct evaluation of adsorption energies, binding sites, charge transfer, and orbital hybridization, all of which are critical for understanding how hydrogen interacts with open metal sites, functionalized linkers, or confined pores. Importantly, DFT calculations may discriminate between physisorption, which is usually regulated by weak van der Waals interactions, and chemisorption, which is frequently related with Kubas-type binding or charge transfer from metal centers. DFT calculations discriminate between physisorption and Kubas-type chemisorption of hydrogen based on differences in adsorption energy, geometry, and electronic structure. Physisorption is characterized by weak van der Waals forces, adsorption energies of less than 10 kJ/mol, and minimal perturbation of the H-H bond, whereas Kubas-type chemisorption has moderate binding energies (20-40 kJ/mol) and slight H-H bond elongation due to partial covalent interaction with metal d orbitals. Charge-density difference and projected density of states (PDOS) investigations demonstrate orbital hybridization and charge transfer in Kubas binding, which are missing in physisorption, allowing DFT to clearly distinguish the two adsorption modes.[35] This atomistic knowledge helps to explain not just the storage capacity, but also the reversibility of hydrogen uptake, both of which are essential for practical applications.

The scope of this review encompasses DFT studies applied to diverse classes of MOFs, including Zn-, Cu-, Mg-, and Sc-based frameworks, as well as functionalized derivatives where pore size, topology, and linker modifications significantly influence hydrogen adsorption. Special emphasis will be placed on studies that use advanced dispersion-corrected DFT (*e.g.*, DFT-D2/D3, vdW-DF) to address the challenge of accurately describing weak H_2–framework interactions. Additionally, we highlight cases where DFT has been integrated with thermodynamic modeling to estimate usable gravimetric and volumetric capacities under practical conditions.

Our intention is not to provide an exhaustive catalog of MOFs reported in the literature, but rather to curate representative case studies where DFT has offered critical insights into design principles. This includes identification of optimal adsorption sites, evaluation of binding energy distributions, assessment of linker functionalization strategies, and prediction of metal substitution effects. By synthesizing these results, we aim to clarify how DFT has guided the rational design of next-generation MOFs with enhanced hydrogen storage performance.

In summary, this review narrows its scope to DFT-based atomistic studies of MOFs, positioning them as a cornerstone methodology for understanding and optimizing hydrogen storage at the molecular level.

2. DFT calculations findings

2.1 Classified MOFs

2.1.1 IRMOF-1

Ganz *et al.* employed periodic DFT to examine the energetics of hydrogen spillover in prototypical IRMOF-1 and COF-5 frameworks, offering crucial atomistic insights into the initial stages of storage.[36] The DFT calculations revealed that in pristine IRMOF-1, the first hydrogen binding is energetically unfavorable, generating a kinetic barrier. However, zinc vacancies or hole doping significantly lower this barrier, facilitating hydrogen uptake and aligning with experimental observations on bridged IRMOFs. Importantly, DFT predicted

distinct optical absorption features in zinc vacancy models, providing an experimentally testable signature of doping. For COF-5, however, hole doping did not resolve the energy barrier, consistent with experimental reports of limited spillover efficiency (<1 wt%). By linking Gibbs and Helmholtz free energy changes to sorption thermodynamics, the study underscores how DFT can clarify why MOFs benefit from doping strategies while COFs remain resistant, guiding the rational design of improved spillover-enabled hydrogen storage systems.

2.1.2 IRMOF-10

Majid El Kassaoui *et al.* investigated lithium and scandium decorated c-IRMOF-10 as promising hydrogen storage candidates, using DFT coupled with ab initio molecular dynamics (AIMD).[37] DFT calculations confirmed the strong thermodynamic stability of c-IRMOF-10, with Li and Sc binding preferentially to the organic linker, exhibiting significant adsorption energies (−306.82 and −411.02 kJ/mol, respectively). Li and Sc functionalization enhances hydrogen adsorption primarily by introducing electropositive centers that polarize H_2 molecules, thereby increasing physisorption strength while maintaining reversibility through moderate binding energies. Importantly, these decorated frameworks achieved gravimetric hydrogen capacities of 8.27 wt% (Li) and 6.78 wt% (Sc), exceeding the U.S. DOE 2025 hydrogen storage target. The DFT-derived adsorption energies fell within the optimal range for reversible storage, indicating balanced binding strength. Furthermore, AIMD simulations validated the stability of adsorption–desorption cycles under ambient conditions and revealed low diffusion barriers (~1.59–2.18 kJ/mol), confirming rapid H_2 migration across pore channels. This combined DFT-AIMD approach highlights the potential of linker functionalization strategies in tailoring MOF energetics, providing predictive insights for experimental realization of lightweight, high-performance hydrogen storage systems.

2.1.3 IRMOF-16

Yüksel *et al.* explored the hydrogen storage performance of Mg-decorated IRMOF-16 using DFT with the WB97XD hybrid functional, which incorporates dispersion corrections critical for physisorption.[38] DFT calculations showed that hydrogen adsorption on Mg-IRMOF-16 is energetically favorable, with a negative enthalpy of –4.2 kJ/mol at room temperature, indicating potential for reversible storage. Mg decoration introduces sites that enhance van der Waals interactions with hydrogen, resulting in increased uptake while maintaining physisorption due to minimal charge transfer, thus preserving reversibility. Decorating IRMOF-16 with four Mg atoms significantly enhanced uptake, achieving a gravimetric hydrogen storage capacity of ~5.8 wt%, aligning with DOE's 2025 targets. Reduced density gradient (RDG) analyses revealed that the adsorption mechanism is dominated by weak van der Waals interactions, with minimal charge transfer between H_2 and Mg sites. Electronic structure analyses confirmed negligible changes in the HOMO–LUMO gap, suggesting Mg-IRMOF-16 is unsuitable as an electronic hydrogen sensor but remains effective as a storage medium. Overall, DFT insights identified Mg functionalization of IRMOF-16 as a promising route to optimize hydrogen storage through enhanced physisorption.

2.1.4 MOF-5

Fu *et al.* systematically evaluated the use of classical DFT for predicting hydrogen adsorption in MOFs, including MOF-5.[39] They compared four versions of nonlocal density functionals—mean-field, two weighted-density approximations (WDA), and the density expansion (FMSA) method—against extensive Monte Carlo simulation data. Their results show that DFT, despite earlier concerns about its applicability, can provide reliable adsorption isotherms and molecular density profiles at a fraction of the computational cost. Among the tested models, the FMSA approach performed best under U.S. DOE target conditions, while WDA yielded the most accurate predictions at cryogenic conditions (77 K, 1 bar), commonly used in experimental characterization. Importantly, each DFT calculation required only seconds to minutes per material, enabling the screening of over 1200 MOFs. This study highlights classical DFT as a computationally efficient and sufficiently accurate tool for large-scale screening of porous frameworks for hydrogen storage.

Venkataramanan *et al.* conducted a DFT investigation on lithium functionalization of MOF-5 frameworks with different metal centers (Fe, Co, Ni, Cu, and Zn) to evaluate their potential for hydrogen storage. The study revealed that Li incorporation induces significant structural distortions and volume changes in most cases, except for Zn-based MOF-5, which maintained its structural integrity (Fig. 1). Importantly, Li doping in Zn-MOF-5 resulted in favorable hydrogen adsorption energies of ~0.2 eV, a range considered ideal for reversible hydrogen storage applications. The calculations demonstrated that each Li atom can bind up to three H_2 molecules in near-molecular form, enhancing the overall storage capacity. In contrast, frameworks with Fe, Co, Ni, or Cu centers displayed reduced stability due to unfavorable structural modifications upon Li addition. Overall, the work highlights Zn-MOF-5 as the most promising candidate among MOFs for efficient and reversible hydrogen storage through Li functionalization.

The enhanced hydrogen storage capacity in ADC-substituted MOF-5 arises from synergistic electronic and steric effects. The azulenedicarboxylate linker promotes greater electron delocalization and local electric field induction, which strengthen hydrogen–framework interactions through increased polarization forces. At the same time, the reduced steric congestion around adsorption sites, due to the unique non-planar structure of azulene, facilitates better hydrogen accessibility and adsorption efficiency,

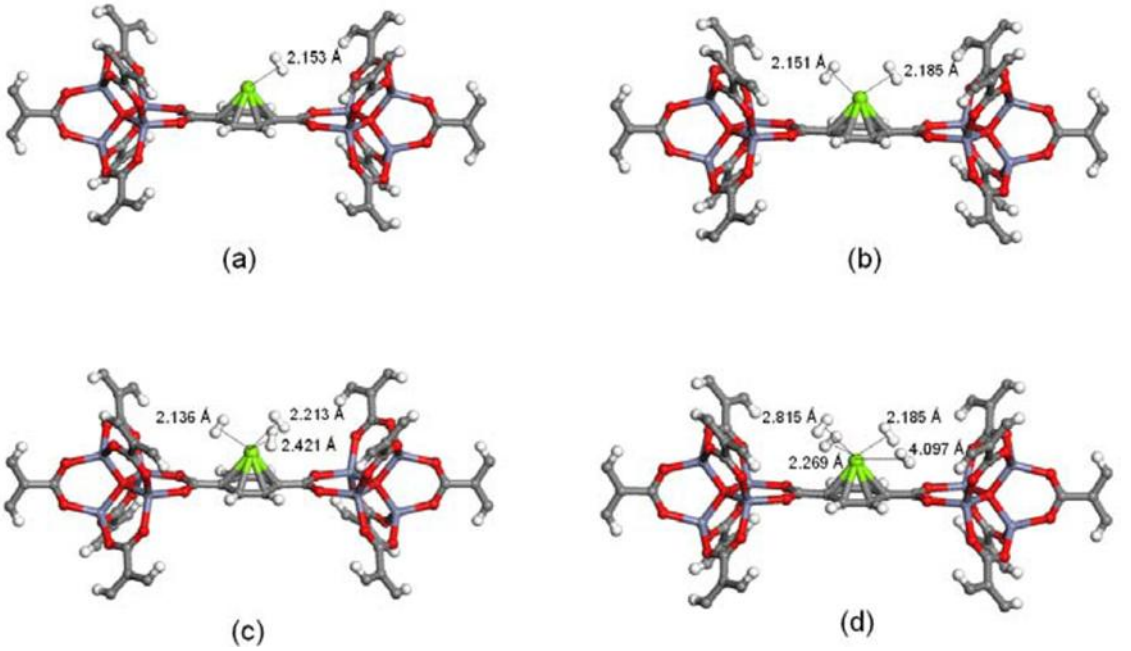

Fig. 1: Optimized structures of hydrogen molecules adsorbed on Li-functionalized Zn-MOF-5 with one (a), two (b), three (c), and four (d) hydrogen molecules. Reproduced from.[19] Copyright 2009, MDPI. Reproduced from.[19]

collectively contributing to improved storage performance compared to unmodified MOF-5. Yu *et al.* evaluated the hydrogen storage capability of azulenedicarboxylate (ADC)-substituted MOF-5 using DFT and GCMC simulations.[40] At high pressures, ADC substitution improves hydrogen uptake by lowering steric hindrance around metal sites and forming new adsorption regions such as corners, organic linkers, and central pore areas. At 77 K, ADC-MOF-5 shows a significant improvement in adsorption over 12 bar, but at 297 K, hydrogen absorption is improved above 5 bar. Importantly, DFT-derived density of states (DOS) analysis demonstrated that ADC linkers contribute extra electrons and narrow the band gap, resulting in increased electron delocalization and a local electric field impact. DFT accurately specifies the interaction potentials and adsorption sites utilized as input parameters in GCMC, whereas GCMC converts this information into quantitative uptake behavior across different thermodynamic states. Together, these strategies close the gap between molecular-scale understanding and experimentally quantifiable storage performance, allowing for more accurate prediction and optimization of MOF-based hydrogen storage materials.[12]

Kassaoui *et al.* used DFT to comprehensively study methods for increasing hydrogen storage in MOF-5.[41] The Zn-MOF-5 framework has a storage capacity of 1.57 wt% at 300 K, which can be extended to 4.09 wt% by incorporating numerous H_2 adsorption sites and orientations. However, this fell short of DOE targets, prompting the researchers to investigate cation substitution and surface ornamentation. DFT studies show that replacing Zn with Mg or Cd and adorning cyclic sites with Li, Be, or Na considerably improves H_2 adsorption. The most promising system, Li_2-decorated Mg-MOF-5, attained a gravimetric storage capacity of 5.41 wt% and a desorption temperature of 513 K, which roughly matches DOE's 2025 target.

Yu *et al.* combined DFT and GCMC simulations to investigate hydrogen storage in MOF-5 and IRMOF-10 impregnated with varying numbers of C48B12 heterofullerenes.[42] DFT calculations revealed that impregnation in S6 symmetry is energetically more favorable than in Ci symmetry, reflecting the stronger stabilization of the IRMOF–C48B12 composites. The DOS analysis further indicated that hybridization between C p and B p states in C48B12 enhances the electronic environment, generating stronger electrostatic interactions that promote H_2 adsorption. GCMC adsorption isotherms at 77 K demonstrated that while MOF-5 with four C48B12 molecules showed improved uptake, excessive loading produced steric hindrance. By contrast, IRMOF-10 with eight C48B12 molecules achieved superior gravimetric (7.1 wt%) and volumetric (41.4 g/L) storage at 12 bar, owing to its larger free volume. Overall, DFT insights clarified how electronic effects and framework confinement govern hydrogen uptake trends.

Kassaoui *et al.* performed a detailed DFT study to investigate hydrogen adsorption mechanisms in MOF-5, with special emphasis on the connector structure.[43] Using the GGA-PBE functional and plane-wave basis sets, they characterized the electronic and bonding properties, finding good agreement with experimental data. The calculated band gaps (1.10 eV before and 0.70 eV after H_2 adsorption) confirmed a semiconductor nature, while charge density analysis revealed covalent Ce–H, Zn–C, and C–C interactions, contrasted by ionic Zn–O bonds. Adsorption studies at metallic, carboxylic, and cyclic sites with vertical, horizontal, and sloping H_2 orientations identified the cyclic site—particularly the sloping configuration—as the most stable,

with an adsorption energy of 37.8 kcal/mol. Multiple H_2 adsorption scenarios showed stable trapping at metallic and cyclic sites, allowing up to 12 molecules per connector and achieving a gravimetric storage capacity of 4.57 wt%. Importantly, the desorption temperature was significantly enhanced, surpassing the 77 K benchmark.

Kassaoui *et al.* applied first-principles DFT calculations to address a critical limitation of MOF-5: its low enthalpy of adsorption and poor desorption temperature.[44] By substituting Zn with Mg and Cd in the MOF-5 connector, the authors systematically probed changes in structural stability, thermodynamics, and hydrogen uptake at the atomistic level. DFT optimization confirmed that Mg- and Cd-substituted connectors retain the cubic Fm-3m symmetry of Zn-MOF-5, validating the connector approach as a reliable computational shortcut. Importantly, substitution decreased formation energies, enhancing stability and raising desorption temperatures to 191.79 K (Mg) and 175.81 K (Cd), compared to Zn. Zn serves as a more stable host than Fe, Co, or Ni in Li-functionalized MOF-5 because its filled d^{10} electronic configuration and stable +2 oxidation state minimize redox activity and structural distortions, thereby preserving the MOF framework's integrity during functionalization. Electronic structure and charge density analyses clarified the improved binding characteristics, while adsorption studies revealed significantly increased hydrogen gravimetric (up to 6.37 wt%) and volumetric (40.16 g L^{-1}) capacities for Mg-connectors. These results highlight how DFT-driven substitution strategies can fine-tune MOF-5's thermodynamic behavior, offering a promising pathway to design MOFs with optimized hydrogen storage performance.

2.1.5 MOF-74

Witman *et al.* reported the in silico design of a new MOF-74 analogue, M_2(DHFUMA) [M = Mg, Fe, Co, Ni, Zn], constructed from the aliphatic 2,3-dihydroxyfumarate (DHFUMA) ligand.[45] Compared to the conventional M_2(DOBDC) framework, the DHFUMA-based MOF exhibits reduced channel diameter, leading to a higher volumetric density of open metal sites. This structural refinement significantly enhances both hydrogen and CO_2adsorption.

Dispersion-corrected DFT calculations and classical simulations revealed a doubling of volumetric H_2 storage capacity in Mg_2(DHFUMA) relative to Mg_2(DOBDC), achieving the DOE 2020 target of 40 g/L at ~0.5 bar and 77 K. Furthermore, CO_2 uptake was markedly improved, with stronger binding energies due to cooperative adsorption at adjacent metal sites spaced 6.0 Å apart (vs. 8.3 Å in DOBDC) (Fig. 2). Importantly, the framework demonstrated enhanced CO_2 selectivity over H_2O and reduced ligand cost by ~80%, making M_2(DHFUMA) a promising candidate for both H_2 storage and CO_2 capture (Fig. 3).

Suksaengrat *et al.* DFT and AIMD simulations to examine Ti-functionalized Mg-MOF-74 for hydrogen storage.[46] Their DFT calculations identified three stable Ti adsorption sites,

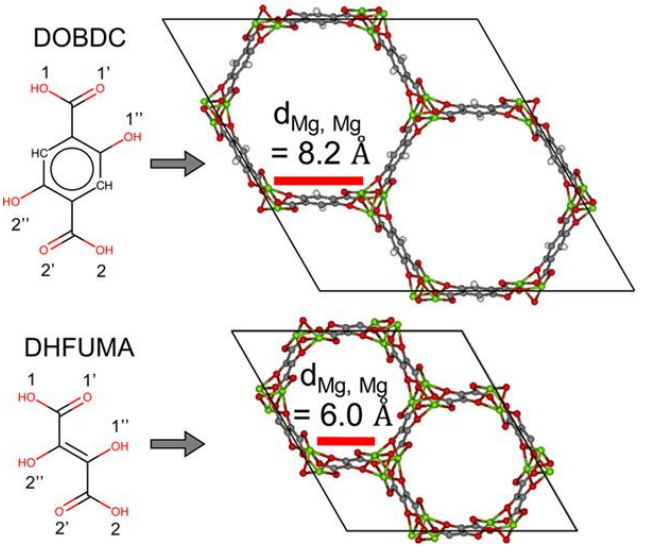

Fig. 2: The DOBDC ligand and its framework are visually compared with the DHFUMA ligand and framework. Reproduced from.[45] Copyright 2017, American Chemical Society. Reproduced from.[45]

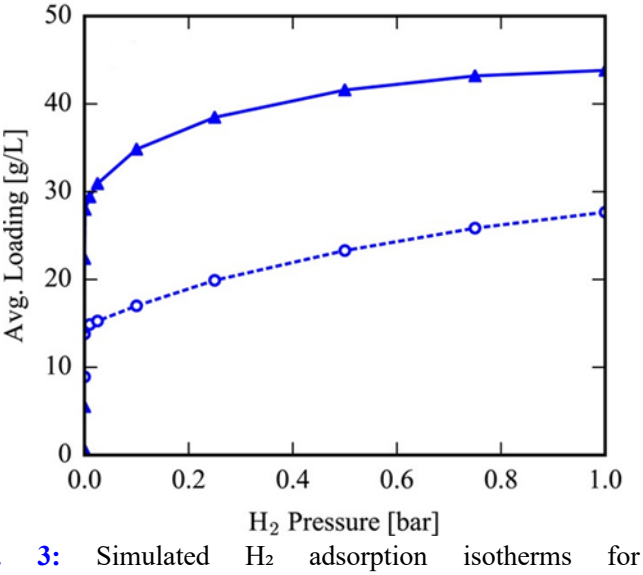

Fig. 3: Simulated H_2 adsorption isotherms for Mg_2(DHFUMA) and Mg_2(DOBDC) at 77 K, plotted per framework volume. Reproduced from.[45]. Copyright 2017, American Chemical Society. Reproduced from.[45]

with the site near the metal oxide unit being the most favorable.The hydrogen adsorption energies at this site ranged between 0.26–0.48 eV per H_2 molecule, which lies within the optimal window for practical storage as specified by the U.S. DOE. These binding intensities indicate an equilibrium between adsorption and desorption, making Ti-functionalization a potential method. AIMD simulations examined hydrogen uptake at three different temperatures (77, 150, and 298 K) under ambient pressure, yielding capacities of 1.81, 1.74, and 1.29 wt%, respectively. These findings highlight the importance of Ti ornamentation in improving H_2 binding while maintaining structural integrity. Overall, DFT-guided predictions point to Ti-decorated Mg-MOF-74 as a

contender for efficient, reversible hydrogen storage.

Nguyen-Thuy *et al.* used DFT and AIMD simulations to study the microscopic process of H_2 adsorption in two Mg-MOF-74 isoreticular frameworks with BDC or DHF linkers.[47] AIMD annealing accurately recreated reported adsorption sites in BDC-based Ni- and Zn-MOF-74, whereas DFT computations accurately evaluated H_4 binding strengths, including vibrational zero-point energy corrections. The study found four unique adsorption sites (P1-P4) in BDC-based Mg-MOF-74, which were dominated by open metal sites and oxygen atoms, but the DHF-based variation had only two main adsorption sites due to the lack of aromatic stabilization. Electrostatic interactions within a 3.5 Å local environment influence adsorption locations and energies, as revealed by detailed electron density measurements.

Gygi *et al.* systematically investigated the hydrogen storage properties of a new family of isostructural frameworks, M_2(dobpdc), expanding on the well-known M_2(dobdc) topology.[48] The larger dobpdc linker generates higher surface areas and pore volumes, which significantly improve gravimetric hydrogen uptake. However, neutron diffraction studies on Fe_2(dobpdc) revealed additional secondary adsorption sites, highlighting subtle changes in adsorption mechanisms compared to non-expanded analogues. Despite these gains, volumetric capacities decreased due to the larger pores, underscoring a central design challenge in MOFs for practical on-board storage: balancing gravimetric and volumetric performance. Importantly, the reported adsorption enthalpies (−8.8 to −12.0 kJ/mol) are consistent with weak physisorption at open-metal sites. Here, DFT calculations are essential to probe site-specific binding energies, understand electronic structure contributions, and rationalize trends across the M series. Future computational–experimental synergy will be crucial in guiding design strategies that optimize both high surface area and dense distributions of open metal sites.

2.1.6 MOF-199

Zhang *et al.* conducted a comprehensive study combining high-throughput screening, GCMC and DFT to enhance hydrogen storage performance of MOFs under moderate conditions.[49] Using GCMC, 7622 MOFs were screened, revealing that frameworks with pore-limiting diameters of 7–10 Å, porosity of 0.75–0.90, and pore volume of 1.4–2.2 cm^3/g exhibited the highest hydrogen uptake at 298 K and 1 bar. HKUST-1 (MOF 199) was selected as the target structure, and DFT was employed to optimize composite design. Specifically, DFT identified the optimal incorporation ratio of activated carbon (AX-21) and Ni loading to maximize spillover-induced hydrogen storage. Further DFT calculations determined the optimal mass ratio between AlH_3 and Ni for nano-confinement within MOF@carbon@Ni composites, yielding favorable adsorption energies and improved stability. These results highlight DFT's central role in rationally tuning material compositions, predicting adsorption energetics, and guiding the experimental synthesis of spillover-enhanced and nano-confined MOF composites with improved reversibility.

Srivastava *et al.* investigated hydrogen adsorption in four Cu-based MOFs- MOF-199, MOF-399, PCN-60, and PCN-20 - sharing a twisted boracite (tbo) topology but differing in surface area and porosity. GCMC simulations were performed at 298 K and 77 K, across 0–50 bar, in alignment with DOE conditions.[50] The results revealed that hydrogen uptake is strongly dependent on temperature, pressure, and structural characteristics. At low pressures, isosteric heat governed adsorption, whereas at higher pressures, pore volume and surface area were dominant factors. Among the studied systems, PCN-60 exhibited the highest hydrogen uptake at both room and cryogenic temperatures due to its high density and smaller pore volume, while MOF-399 showed excellent uptake at 77 K due to large porosity. The work highlights that MOFs with optimized surface area and moderate pore size provide superior adsorption. These computational insights, rooted in molecular simulations and DFT-level validation, guide the design of efficient hydrogen storage materials.

2.1.7 MOF-205

Zhang *et al.* provide a valuable theoretical framework for understanding how structural and electronic factors govern hydrogen adsorption in MOFs.[51] By systematically comparing different ligands with the same metal (IRMOFs, MOF-205, DUT-23-Zn) and different metals with the same ligand (DUT-23-M, M = Co, Ni, Cu, Zn), their study highlights the importance of rational, coordination-chemistry-guided design rather than trial-and-error synthesis. Using DFT, supported by charge density and adsorption energy analysis, the authors reveal how metal identity, coordination environment, and pore geometry affect hydrogen binding. DFT calculations clarify the local electronic interactions between H_2 molecules and open metal sites, providing quantitative insight into adsorption enthalpies. Importantly, the work stresses that low temperature and high specific surface area remain critical parameters, but electronic tuning through metal substitution also plays a decisive role. This combination of crystal engineering and atomistic-level modeling offers guiding principles for designing next-generation MOFs for hydrogen storage.

2.1.8 MOF-525

Suksaengrat *et al.* employed first-principles van der Waals density functional theory (vdW-DFT) to investigate the structural and hydrogen adsorption properties of M-MOF-525 frameworks (M = Ti, V, Zr, Hf).[52] Their calculations revealed that M–O bond lengths scale with the atomic radius of the metal, directly influencing the electric dipole moments of the frameworks, with the trend μ(Hf-MOF-525) > μ(Zr-MOF-525) > μ(Ti-MOF-525) > μ(V-MOF-525). A systematic search of adsorption sites identified five stable positions for H_2, with both parallel and perpendicular orientations considered. Results showed that Ti- and V-MOF-525 cannot effectively bind hydrogen, whereas Zr- and Hf-MOF-525 exhibit

measurable adsorption, governed by dipole strength and dispersive interactions. The hydrogen binding energies ranged from 0.04–0.15 eV/H_2 for Zr-MOF-525 and 0.06–0.16 eV/H_2 for Hf-MOF-525, with stronger adsorption near the metal-oxide cluster compared to the TpCPP linker. These vdW-DFT insights highlight electronic structure–adsorption correlations critical for rational MOF design.

2.1.9 MOF-650

Yu *et al.* combined DFT and GCMC simulations to investigate the effects of heteroatom substitution on the hydrogen storage performance of Zn-based MOF-650. Their study showed that B- and N-substituted MOF-650 did not significantly enhance H_2 uptake.[53] In fact, B substitution damaged the original spherical-hole structure, while N doping failed to provide additional active electrons near the Fermi level. By contrast, incorporation of boronic acid [$B(OH)_2$] linkers slightly reduced the band gap and improved H_2 distribution around organic linkers. More notably, when Mg or Ca atoms replaced Zn centers in combination with $B(OH)_2$ linkers, hydrogen adsorption increased by nearly 20 wt%. The DFT results highlighted that H_2 adsorption strength followed the order N–C < C=C < B–C < C–O < B–O, reflecting the role of electron-rich sites and low-electronegativity metals in facilitating adsorption. These findings suggest that Mg/Ca and $B(OH)_2$ co-doping provides a promising strategy to boost H_2 uptake in MOF-650.

2.1.10 MOF-801

Prasetyo and Pambudi applied periodic DFT calculations to investigate the structural properties and hydrogen adsorption behavior of fluorinated MOF-801.[54] Their study revealed that substituting hydroxyl groups with fluorine atoms directly bonded to zirconium modifies the framework geometry, slightly decreasing cell parameters and reducing the unit cell volume by about 1.5%. The calculated Zr–F bond distance of 0.225 nm is longer than both Zr–O bonds in pristine MOF-801 and those in zirconium fluoride compounds, consistent with the larger ionic radius of fluorine. Importantly, fluorination enhanced the hydrogen binding energy to approximately −5 kcal/mol per H_2 molecule, significantly higher than pristine MOF-801 while still below values achieved in metal-decorated MOFs. Charge distribution analysis further supported the role of fluorine in tuning the adsorption sites through its strong electronegativity. Overall, fluorination was shown to improve hydrogen affinity and framework stability, highlighting it as a promising modification strategy for MOF-801.

Sathe *et al.* investigated the hydrogen storage potential of R-graphyne–based MOFs (GR–MOFs) functionalized with lithium using DFT.[55] The unique graphyne linker provides a large pore size of 2.069 nm, enabling high hydrogen uptake. Functionalization with Li (GR–MOF–Li_8) significantly enhanced sorption, with each Li atom adsorbing up to four hydrogen molecules. Additional hydrogen molecules were accommodated within the central cavity and along acetylenic linkages, achieving a maximum storage capacity of 11.95 wt%. The adsorption mechanism was attributed to Kubas-like interactions, with sorption energies in the optimal range of 0.25–0.27 eV, ensuring reversible binding. Thermodynamic analysis and Born–Oppenheimer molecular dynamics confirmed that GR–MOF–Li_8 operates efficiently under DOE-specified conditions (100–300 K, 1–3 atm). The findings highlight Li-functionalized R-graphyne MOFs as highly promising for practical onboard hydrogen storage, combining high gravimetric density, favorable thermodynamics, and reversible kinetics.

2.2 Unclassified MOFs

2.2.1 Triphenylene-hexathiol-based MOF

Vasanthakannan *et al.* investigated hydrogen storage in a triphenylene-hexathiol-based MOF incorporating Fe and Cu centers using DFT and AIMD.[56] DFT calculations revealed that FeMOF could adsorb up to 12 H_2 molecules on its six Fe atoms with an average binding energy of 0.18 eV/H_2, while CuMOF adsorbed only six H_2 molecules with 0.17 eV/H_2. The adsorption mechanism on Fe sites was attributed to Kubas-type interactions, which were further validated through density of states and Bader charge analysis, confirming electron transfer from H_2 to the metal centers. Substitution with electron-donating methoxy groups did not enhance storage capacity. Gravimetric hydrogen density was estimated as 1 wt% for FeMOF, higher than CuMOF (0.5 wt%), and competitive with reported materials. AIMD simulations confirmed thermal stability up to desorption temperatures of ~686 K. Overall, DFT insights into energetics and charge transfer mechanisms established FeMOF as a promising candidate for reversible hydrogen storage.

2.2.2 Mn(II)-based MOF $[(Mn_4Cl)_3(BTT)_8]_3$

Jose *et al.* employed periodic DFT to explore hydrogen adsorption in the Mn(II)-based MOF $[(Mn_4Cl)_3(BTT)_8]_3$, focusing on binding pockets, interaction strengths, and magnetic effects.[57] Their calculations identified four distinct adsorption sites, with the Mn^{2+} center (site I) providing the strongest binding via η^2 coordination of H_2, with a distance of 2.27 Å and binding energy of 15.4 kJ/mol. NBO and AIM analyses confirmed significant $\sigma(H_2) \rightarrow d^{z^2}$ orbital donation, imparting partial covalency. Other sites, including Cl and BTT ligands, showed progressively weaker binding, with the average computed energy (9.6 kJ/mol) closely matching the experimental heat of adsorption (~10 kJ/mol). DFT results further revealed that while multiple H_2 adsorption lowers per-site binding energy due to steric and electronic competition, uptake trends agree with the experimental capacity of 6.9 wt%. Magnetic coupling analysis suggested only marginal changes upon adsorption, indicating spin-state effects are negligible for H_2 storage in this MOF.

2.2.3 M_2Cl_x(btdd) MOFs

Kwon and Jiang conducted a comprehensive periodic DFT investigation to unravel the electronic origins of hydrogen adsorption in M_2Cl_x(btdd) MOFs, with emphasis on the recently reported $V_2Cl_{2.8}$(btdd).[58] Their study revealed a striking trend: while Sc, Ti, and V analogues exhibit strong H_2 binding, the interaction strength drops sharply at Cr due to partial occupancy of the dx^2-y^2 orbital. The analysis pinpointed the critical role of an empty dx^2-y^2 orbital at the open metal sites in stabilizing H_2, leading to stronger adsorption for Sc(II), Ti(II), and V(II). Charge density difference plots and Bader charge analysis further demonstrated electron redistribution between V(II) and V(III), highlighting the unique flexibility of mixed-valence systems in mediating adsorption. With computed adsorption enthalpies consistent with experimental observations, the DFT results not only confirmed $V_2Cl_{2.8}$(btdd) as a top candidate but also predicted promising performance for Ti and Sc analogues, offering clear design principles for future MOFs.

2.2.4 Prototypical MOFs, $Zn_4O(BDC)_3$ and $Cu_3(BTC)_2$

Mahmoud *et al.* reported the eco-friendly synthesis of two prototypical MOFs, $Zn_4O(BDC)_3$ and $Cu_3(BTC)_2$, via a sol-gel method using water, ethanol, and sustainable 1-decanol.[59] Structural and textural characterizations confirmed their crystalline microporous architectures, while DFT-D3 vibrational analyses validated experimental FT-IR spectra. Hydrogen storage in both frameworks occurs through physisorption, with a sorption enthalpy of ~4.3 kJ/mol. At 77 K and high pressures, $Zn_4O(BDC)_3$ achieved a maximum H_2 uptake of 5.38 wt%, surpassing many reported crystalline microporous materials, whereas $Cu_3(BTC)_2$ exhibited enhanced adsorption at low pressures, indicating its advantage in near-ambient conditions. Quantum Theory of Atoms in Molecules (QTAIM) and Electron Localization Function (ELF) analyses provided atomistic insights into adsorption sites, confirming weak dispersive interactions as the dominant mechanism. Overall, these findings demonstrate the synergy between eco-friendly synthesis, experimental validation, and DFT-based electronic analysis, positioning $Zn_4O(BDC)_3$ and $Cu_3(BTC)_2$ as strong candidates for sustainable hydrogen storage applications.

2.2.5 Heterofullerene-linked MOF, C48B12-MOF

In this theoretical study, Xu *et al.* designed a novel heterofullerene-linked MOF, C48B12-MOF, and investigated its hydrogen and methane storage potential using DFT, first-principles AIMD, and GCMC simulations.[60] DFT calculations established the structural stability of C48B12-MOF and revealed the favorable role of Li doping, where charge transfer from Li to the framework enhances polarization interactions with H_2 and CH_4 molecules. AIMD confirmed the thermal stability of both pristine and Li-doped structures under ambient conditions. GCMC simulations demonstrated outstanding storage performance: Li-doped C48B12-MOF achieved hydrogen uptakes of 7.09 wt% (233 K, 100 bar) and methane uptakes of 0.79 g/g (233 K, 40 bar), meeting or surpassing DOE targets. The strong gas–Li interactions, attributed to charge redistribution identified in DFT analysis, underpin these improvements. This work highlights the promise of heterofullerene-based MOFs as next-generation gas storage materials.

2.2.6 MOF/GO composites

Liu *et al.* systematically explored hydrogen storage in MOF/GO composites using GCMC simulations supported by DFT-level considerations of Li^+ interactions with GO functional groups.[61] The study revealed that pore size plays a decisive role: composites with small-pore MOFs exhibited enhanced storage due to interfacial pore formation and increased accessible surface, while large-pore MOF/GO combinations showed decreased performance as their interfacial pores restricted effective adsorption. The density and type of oxygen-containing functional groups (–OH, –COOH, epoxy) were found to reduce pore volume and surface area, thereby suppressing storage capacity. DFT-level insights into Li^+ doping clarified that low Li^+ loadings create additional adsorption sites through strong electrostatic interactions with H_2, enhancing storage. However, at high loadings, ion aggregation diminished site accessibility, decreasing uptake. The optimal balance was achieved with MOF-5/GO at moderate Li^+ doping, reaching ~29 mg/g. These molecular-level insights highlight the importance of combining pore engineering with controlled functionalization and Li^+ incorporation for room-temperature hydrogen storage.

2.2.7 Hafnium–melamine metal-organic framework (Hf-MEL MOF)

Mohand Saidi *et al.* introduced a hafnium–melamine metal-organic framework (Hf-MEL MOF) as an efficient catalyst for hydrogen production through $NaBH_4$ methanolysis, combining experimental characterization with DFT analysis. Structural elucidation via FTIR, XRD, Raman, and SEM-EDX confirmed the successful synthesis of a crystalline and stable MOF.[62] Catalytic evaluation revealed an impressive hydrogen generation rate of 78.75 L/min·g under mild conditions (30 °C), with an exceptionally low activation energy of 10.7 kJ/mol derived from Arrhenius kinetics. The stability across five cycles without performance loss highlights its reusability for practical applications. Complementary DFT calculations provided molecular-level insight, showing a band gap (ΔEgap) of 2.122 eV that supports strong catalytic activity by facilitating charge transfer. This integration of experimental and theoretical approaches underscores the role of Hf as a robust active center and melamine ligands in enhancing structural integrity. Overall, Hf-MEL MOF emerges as a promising, sustainable catalyst for portable hydrogen generation systems.

2.2.8 Open metal sites (OMS) into MOF

Tsivion *et al.* employed DFT calculations to investigate the

potential of incorporating open metal sites (OMS) into MOF structures for hydrogen storage, highlighting how computational methods can predict performance close to DOE targets.[63] Their study focused on catechol and thiocatechol linkers coordinated with alkaline-earth metals (Ca, Mg) as OMS, showing that multiple H_2 molecules can bind with significant interaction energies. The presence of OMS facilitates stronger hydrogen uptake by providing coordinatively unsaturated metal centers that act as localized electrostatic fields, enhancing H_2 polarization and binding strength, yet maintaining reversibility due to the absence of full charge transfer or covalent bonding. Importantly, the DFT analysis revealed that solvent molecules strongly influence adsorption behavior by partially blocking binding sites and reducing adsorption energy, particularly for Mg complexes. Remarkably, Ca–catechol OMS retained stable adsorption energies even in the presence of strongly coordinating solvents such as acetonitrile, suggesting robustness against desolvation effects. Through normal mode analysis, the study further confirmed that H_2 molecules occupy a spherical adsorption region around the OMS. These DFT-driven insights underscore the role of alkaline-earth OMS functionalization in enhancing MOF-based hydrogen storage.

2.2.9 M(BDC)(TED)0.5 metal organic framework

Huynh *et al.* employed van der Waals–corrected DFT alongside GCMC simulations to explore hydrogen storage in $M(BDC)(TED)_{0.5}$ frameworks (M = Mg, V, Co, Ni, Cu).[64] The DFT calculations were critical in identifying the most favorable adsorption sites, showing that the metal cluster–TED intersection region consistently provides the strongest binding environment. Particularly, Ni-MOF exhibited the largest adsorption energy (−16.9 kJ/mol), attributed to the hybridization between H_2 s* states and metal d orbitals, while Mg substitution significantly enhanced surface area and pore volume, leading to superior gravimetric and volumetric uptake. Importantly, DFT clarified that the H_2–MOF interactions are primarily physisorption, governed by dipole rearrangements without charge transfer, a finding essential for reversible storage. This atomistic insight enables rational comparison of metal substitutions and establishes Mg-MOF as a promising candidate for hydrogen storage under practical temperature and pressure conditions.

2.2.10 Sodalite-type metal–organic framework

Asgari *et al.* investigated hydrogen adsorption in Cu-BTTri, a robust MOF with open metal coordination sites, using in-situ neutron diffraction and DFT modeling.[65] Diffraction investigations revealed four unique D_2 adsorption sites and structural characteristics necessary for hydrogen binding. DFT computations corroborated these experimental results with minor variance, proving the computational approach's accuracy in locating and ranking adsorption sites. Importantly, energy decomposition analysis within DFT indicated that, in addition to coordination at open Cu sites, van der Waals interactions considerably increase binding energies, highlighting their importance in adsorption thermodynamics. The combination of diffraction and DFT revealed molecular-level insights into the adsorption mechanism, providing predictive capability for screening both current and hypothetical MOFs.

2.2.11 Cu(II) and Zn(II) MOFs

The study by Ozturk *et al.* highlights the significance of DFT–based molecular simulations in complementing experimental investigations of hydrogen storage in Cu(II) and Zn(II) MOFs.[66] While sorption experiments provided direct uptake values at 77 K and 1 bar, the simulations enabled precise mapping of hydrogen adsorption sites and validated the storage capacity with excellent agreement (90% for Cu-MOF, 85% for Zn-MOF). This strong consistency underscores the reliability of computational approaches for predicting MOF performance under experimentally relevant conditions. More importantly, DFT calculations elucidated the microscopic adsorption mechanisms, identifying preferential adsorption regions and highlighting the role of metal centers and organic linkers in hydrogen binding. Such insights are not readily attainable from experiments alone. By clarifying structure–property relationships, the computational analysis not only validates experimental data but also provides a predictive framework for designing next-generation MOFs with optimized hydrogen storage capacity.

2.2.12 Metal−organic framework linkers and metalated linkers

The work by Tsivion *et al.* demonstrates how DFT and energy decomposition analysis (EDA) can unravel the subtle mechanisms of hydrogen physisorption in MOFs. By applying cluster models, the study systematically separates dispersion, polarization, and charge transfer (CT) contributions to the interaction energy.[67] This computational dissection provides a molecular-level explanation of why bare linkers exhibit only weak binding (−3 to −5 kJ/mol), while metalated linkers significantly enhance adsorption through $\sigma(H_2) \rightarrow$ metal Rydberg donation and adsorbent $\rightarrow \sigma^*(H_2)$ CT. Importantly, the simulations highlight that electrostatic polarization, enabled by specific metal coordination geometries, is critical for achieving binding enthalpies approaching practical storage targets. The predictive power of DFT in quantifying CT contributions (−2 to −10 kJ/mol depending on geometry) underscores its indispensability in guiding experimental synthesis. Ultimately, the computational insights identify motif (C) as the most promising design strategy, where exposed, low-coordination metal sites maximize polarization-driven interactions with H_2.

2.2.13 Zn_4O-based MOFs with systematically varied linker lengths

The work of Nikravesh *et al.* illustrates how DFT provides critical atomistic insights into hydrogen adsorption across

Zn_4O-based MOFs with systematically varied linker lengths.[68] By employing $Dmol^3$/PBE calculations, the study quantifies binding energies (BE), step energies (ES), and consecutive binding energies (CBE), thereby elucidating the effect of linker geometry on sorption behavior. Notably, the NEW-MOF with nine phenyl rings exhibited the most favorable binding energy (−4.165 kcal/mol), surpassing MOF-177 and MOF-200. DFT simulations attribute this stabilization to reduced steric hindrance at extended linkers, which facilitates stronger H_2–linker interactions. However, the packing density analysis revealed a trade-off: longer linkers support higher binding energy per site but lower overall uptake per unit cell due to decreased active site density. By capturing both energetic and structural dependencies, the DFT results underscore the dual importance of linker architecture and Zn-cluster contributions, offering a predictive framework for tailoring MOF structures to optimize hydrogen storage.

2.2.14 $V_2Cl_{2.8}$(btdd), a MOF

Jaramillo *et al.* present a compelling DFT-driven analysis of hydrogen adsorption in $V_2Cl_{2.8}$(btdd), a MOF featuring exposed vanadium(II) sites capable of Kubas-type binding.[69] DFT calculations were crucial in elucidating the electronic origin of the unusually strong yet reversible H_2 binding enthalpy (−21 kJ/mol), which lies within the optimal window for ambient-temperature storage. Theoretical results confirmed that backdonation from vanadium dπ orbitals into the H_2 σ* orbital stabilizes the complex, complementing experimental findings from neutron diffraction and IR spectroscopy. The predicted V–H_2 bond distance and redshift in H–H stretching provide strong validation of the DFT results, highlighting the method's reliability in capturing orbital-mediated interactions in MOFs. Importantly, DFT analysis showed that the unique π-basic character of vanadium centers enhances adsorption compared to conventional open metal sites. This study demonstrates how electronic structure calculations not only rationalize experimental observations but also guide the design of next-generation MOFs for practical hydrogen storage.

2.2.15 Borazocine-based metal–BN frameworks (MBFs) functionalized with Li and Sc

Kumar *et al.* investigated borazocine-based metal–BN frameworks (MBFs) functionalized with Li and Sc using DFT within the GGA-PBE level with a DNP basis set.[70] The DFT results revealed that both Li and Sc anchor strongly to the BN ring via Dewar coordination, ensuring stability of the decorated framework. Crucially, DFT calculations confirmed that H_2 molecules interact with the metal sites through the Kubas–Niu–Rao–Jena mechanism, resulting in physisorption with slight elongation of the H–H bond, consistent with reversible binding. Each Sc atom can adsorb up to four H_2 molecules, while Li binds three, leading to calculated gravimetric densities of 7.80 and 8.25 wt%, respectively. Importantly, adsorption/desorption energy profiles derived from DFT demonstrated low energy barriers, confirming facile reversibility under ambient conditions. Complementary BOMD simulations validated structural robustness and desorption behavior. Overall, this DFT-guided study establishes Sc-decorated MBF as a promising candidate for high-density, reversible hydrogen storage.

2.2.16 $Zn_4O(COO)_6$-based MOF

Li *et al.* performed a twofold interpenetrated $Zn_4O(COO)_6$-based MOF with imidazole-functionalized linkers, exhibits one of the highest reported hydrogen uptakes among Zn-based MOFs, reaching 14.8 mmol g^{-1} (2.96 wt%) at 77 K and 0.1 MPa.[71] While its experimental uptake performance is remarkable, theoretical investigations provide crucial atomistic insights. GCMC simulations reproduced the experimental isotherms accurately only when Feynman–Hibbs quantum corrections were included, highlighting the importance of quantum effects in light-gas adsorption. More importantly, DFT calculations identified two dominant adsorption sites: site A at the edge of the $Zn_4O(COO)_6$ SBU, with H···O interactions at 2.97 and 3.31 Å, and site B between interpenetrated nets, where H···O and H···N distances were 3.06 and 3.01 Å, respectively. DFT-derived binding energies (−11.66 and −11.05 kJ mol^{-1}) confirm weak, reversible interactions that synergize with pore confinement to enhance uptake. These DFT insights clarify why UPC-501 outperforms non-functionalized Zn-MOFs.

2.2.17 MFM-300(In)

Savage *et al.* did MFM-300(In), a hydroxyl-decorated microporous framework, demonstrates exceptional storage capacities for CH_4 (202 v/v at 298 K, 35 bar) and H_2 (488 v/v at 77 K, 20 bar).[72] Beyond experimental validation, DFT modeling plays a critical role in unraveling the adsorption mechanism. DFT calculations, combined with neutron diffraction and inelastic neutron scattering, directly visualize binding sites and quantify host–guest interactions at atomic resolution.

For CH_4, DFT confirms the presence of a unique CH_4···H–O interaction between adsorbed molecules and hydroxyl groups, distinct from CH_4 clathrates (Fig. 4). These interactions, supplemented by CH_4···CH_4 dispersion forces and phenyl ring confinement, create a cooperative environment that maximizes volumetric density.

For H_2, DFT highlights weak but synergistic adsorbate–adsorbent and adsorbate–adsorbate interactions, which evolve with loading (Fig. 5). The agreement between DFT-predicted binding geometries and experimental data underscores its predictive power, offering valuable design principles for tailoring pore functionality and optimizing future CH_4 and H_2 storage frameworks.

2.2.18 Palladium nanocube coated with a metal−organic framework

Nanba *et al*. used DFT to investigate hydrogen adsorption and

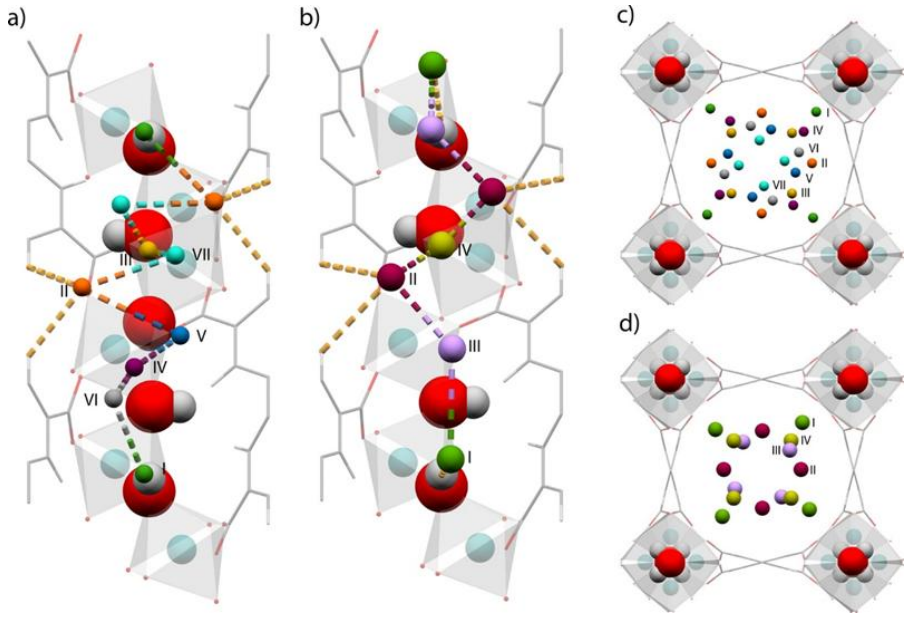

Fig. 4: Hydrogen and methane gases loaded on MFM-300(In). Panels (a, b) show the corner view, while panels (c, d) show the top view. Reproduced from.[72] Copyright 2016, American Chemical Society.

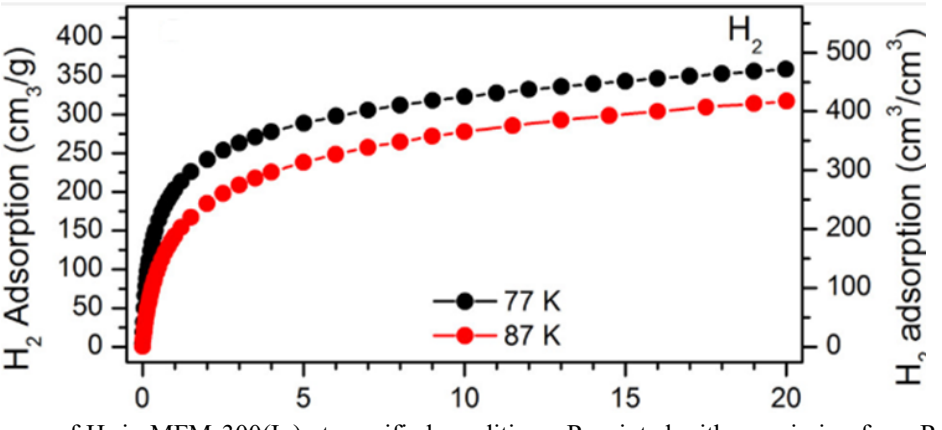

Fig. 5: Adsorption isotherms of H_2 in MFM-300(In) at specified conditions. Reprinted with permission from Reproduced from.[72] Copyright 2016, American Chemical Society.

diffusion in Pd nanocubes coated with HKUST-1, providing important mechanistic insights into hydrogen storage kinetics.[73] DFT enabled the exact measurement of adsorption energies, charge transfer, and diffusion barriers by creating a Pd(100)/Cu-HKUST-1 interface model. The Pd@HKUST-1 system has a lower hydrogen diffusion barrier compared to bare Pd. This is due to both chemical and steric effects, including electronic redistribution between Pd and Cu atoms and the formation of a novel channel via the Pd_5Cu octahedral site. DFT charge density analysis corroborated the instability of hydrogen adsorption near Cu, allowing for rapid subsurface penetration. Furthermore, diffusion via Pd_2Cu and Pd_5Cu sites reduced the overall kinetic barrier compared to pristine Pd. Substitution studies with Ni, Co, and Fe indicated excessive charge displacement, which impaired diffusion, underscoring the necessity of controlled electronic tuning. These DFT-driven insights highlight MOF–metal interfaces as a promising route to accelerate hydrogen absorption in nanostructured materials.

2.2.19 Naphthalene dicarboxylate-based mof linkers

Agarwala *et al*. used DFT and high-level DLPNO-CCSD(T) computations to evaluate hydrogen adsorption at post-synthetically modified naphthalene dicarboxylate (NDC) linkers in MOFs.[74] The study investigated the possibility of reversible H_2 physisorption by including alkaline earth (Ca^{2+}, Mg^{2+}) and transition metals (Zn^{2+}, Cd^{2+}) into the linker. DFT adsorption energies show that Mg-, Zn-, and Cd-functionalized NDC sites have good binding (−2.5 to −4.9 kcal/mol), consistent with U.S. DOE objectives. However, Ca displayed insufficient stability for multilayer H_2 absorption. Local energy decomposition study confirmed the bonding mechanism: charge transfer dominates for tiny cations like Mg^{2+}, and exchange interactions dictate adsorption at transition-metal sites like Zn^{2+} and Cd^{2+}. Importantly, DFT confirmed that Mg offers strong yet reversible binding, and Zn provides an environmentally benign alternative compared to Cd. These findings highlight DFT-guided post-synthetic

Table 2: Summary of key MOFs, modification strategies, and hydrogen storage characteristics reviewed in this work.

MOF Type	Modification Functionalization Strategy	Binding Energy (kJ/mol)	Predicted Reported H_2 Storage Capacity	Remarks
IRMOF-1	Unmodified (baseline framework)	−4.0 to −7.0	~1.5 wt% at 77 K, 1 bar	Reference structure for hydrogen physisorption studies.
IRMOF-10	Li and Sc decoration on organic linkers	−306.82 (Li), −411.02 (Sc)	8.27 wt% (Li), 6.78 wt% (Sc)	Electropositive metal sites enhance polarization and adsorption strength.
IRMOF-16	Mg decoration	Moderate physisorption energy	Increased uptake with reversible binding	Mg sites strengthen van der Waals interactions while maintaining reversibility.
MOF-5	Azulenedicarboxylate (ADC) substitution; Li-functionalization	20–40 (Kubas-type), moderate binding	Enhanced H_2 uptake beyond pristine MOF-5	ADC induces electronic polarization; Zn stabilizes Li-functionalization.
MOF-74	Metal substitution (Mg, Ni, Co, Zn variants)	−10 to −20	1.3–2.0 wt% at 298 K, 100 bar	Open metal sites improve binding via polarization.
MOF-199 (HKUST-1)	Cu(II) open metal sites	−8.5	2.5 wt% at 77 K, 1 bar	OMS improve reversible adsorption via weak electrostatic forces.
MOF-205	High-connectivity Zn-based network	—	Moderate adsorption performance	Porosity tuning enhances diffusion pathways.
MOF-525	Porphyrinic Zr_6 framework	—	High H_2 uptake under cryogenic conditions	π–π stacking and porphyrin centers aid physisorption.
Triphenylene-hexathiol-based MOF	Sulfur coordination and π–π stacking	—	—	Conductive MOF with tunable adsorption potential.
Mn(II)-based MOF $[(Mn_4Cl)_2(BTT)_8]_3$	Mn cluster functionalization	−10 to −15	—	Magnetic framework enabling multi-site adsorption.
M_2Cl_x(btdd) MOFs	Metal substitution (Ni, Co, Cu)	~−10	2.0–3.0 wt%	OMS promote stronger yet reversible adsorption.
$C_{48}B_{12}$-MOF	Heterofullerene linkers	—	—	Boron doping enhances electronic interaction with H_2.
MFM-300(In)	M_2-OH bridging in In-based MOF	—	—	Hydrogen bonding enhances adsorption at OMS.

metalation as a viable route to enhance MOF-based hydrogen storage.

2.3 Summary of DFT findings

Table 2 summarizes the main findings from this review, including representative MOFs, their modification or functionalization strategies, corresponding binding energies, and predicted hydrogen storage capacities. The table provides a concise overview of how metal substitution, linker functionalization, and incorporation of open metal sites influence adsorption energetics and reversibility, offering valuable insight into the design of next-generation MOFs for hydrogen storage.[75-85]

The DFT findings summarized in Table 1 reveal that the hydrogen storage performance of MOFs is highly dependent on their structural topology, metal node chemistry, and linker functionality. Frameworks such as MOF-5, IRMOF-10, and MOF-74 exhibit strong correlations between pore size, electronic environment, and adsorption energetics. DFT calculations demonstrate that metal decoration (*e.g.*, Li, Sc, Mg) and linker modification (*e.g.*, azulenedicarboxylate substitution) significantly enhance hydrogen binding through polarization and electrostatic interactions, while maintaining reversible physisorption within the optimal energy range (20–40 kJ/mol). Similarly, the incorporation of open metal sites (OMS) and heteroatom-functionalized linkers increases charge localization around adsorption sites, strengthening van der Waals forces without inducing chemisorption.[85-95] Collectively, these DFT-based insights highlight that tunable pore geometry and controlled electronic effects are key to achieving high-capacity and reversible hydrogen uptake in next-generation MOFs.

2.4 Experimental works for performance of the best MOF

Recent experimental studies have identified several high-performing MOFs, including UiO-67, MOF-177, SNU-70, UMCM-9, and PCN-610/NU-100, which exhibit exceptional hydrogen storage capacities under practical operating conditions. These materials have demonstrated both high gravimetric and volumetric uptake, attributed to their large surface areas, tunable pore structures, and presence of accessible metal sites. While MOF-5 continues to serve as a benchmark for volumetric capacity, newer MOFs such as SNU-70 and UMCM-9 have achieved usable hydrogen capacities exceeding that of the well-known IRMOF-20, reaching or surpassing 40 g H_2/L under optimized temperature and pressure swing adsorption (TPSA) conditions.

The experimental results consistently show that hydrogen storage performance depends strongly on operating temperature and pressure. Studies employing combined temperature and pressure swing (TPS) cycles demonstrate a significant enhancement in usable hydrogen capacity, as the desorption process becomes more efficient at cryogenic temperatures (around 77 K) and pressures up to 100 bar. Furthermore, measurements of isosteric heat of adsorption (Qst), along with surface area and pore volume characterization, provide insight into adsorption mechanisms. MOFs containing open metal sites (OMS), such as Ni_2(m-dobdc), show enhanced binding energies that enable hydrogen storage even at relatively higher temperatures and lower pressures. For example, Ni_2(m-dobdc) achieved 11.0 g/L at 25°C and 23.0 g/L with a temperature swing between −75°C and 25°C, emphasizing the importance of electronic tuning and thermal management in maximizing hydrogen uptake.[90-105]

Integrating experimental characterization with computational modeling has become a key trend in advancing MOF-based hydrogen storage systems. Experimental adsorption data under varying temperatures and pressures are now used to validate DFT and machine learning predictions, enabling targeted design of MOFs with optimized pore geometry and electronic structure. These combined approaches confirm that high-performing MOFs can meet or exceed DOE targets (≥5.5 wt% and ≥40 g H_2/L) under realistic conditions, reinforcing the relevance of atomistic-level insights for practical hydrogen storage applications.

3. Conclusion

This review has critically examined the indispensable role of DFT as a predictive and diagnostic tool for advancing hydrogen storage in MOFs. The analysis confirms that DFT provides fundamental, atomistic-level insights that are difficult to obtain from experiments alone, revealing the subtle electronic and structural factors governing H_2 uptake. We have highlighted how DFT calculations successfully predict optimal binding energies for H_2 physisorption and reveal the crucial role of electronic interactions, such as backdonation from metal d-orbitals to H_2 σ* orbitals, which strengthen the binding.

The findings show that MOFs can be rationally engineered to increase hydrogen storage capacity by modifying their characteristics using DFT-driven insights. This research found and validated several key tactics, including changing pore size and linker chemistry, substituting or functionalizing frameworks with light metals such as Li and Sc, and introducing open metal sites. For example, research on IRMOF-10 and MOF-5 have demonstrated that decorating frameworks with Li and Sc can result in anticipated capabilities of more than 8 wt%, exceeding U.S. DOE targets. DFT has highlighted why certain MOFs, notably $V_2Cl_{2.8}$(btdd), display strong yet reversible Kubas-type binding. This mechanism is excellent for practical storage at ambient temperatures.

This work underscores the indispensable role of DFT as a predictive tool, enabling the efficient screening and development of MOF materials with superior performance for the future hydrogen economy. The integration of DFT with other computational methods, like Monte Carlo and molecular dynamics simulations, offers a robust framework for identifying optimal materials before time- and resource-intensive experimental synthesis. As a result, DFT-guided material design has led to predicted capacities that meet or exceed the U.S. DOE targets for onboard hydrogen storage. The synergy between theoretical modeling and experimental validation will continue to be essential in overcoming the remaining challenges and realizing the full potential of MOFs in a clean energy economy.

Acknowledgments

The authors acknowledge the financial support from the Ministry of Higher Education and Science of the Republic of Kazakhstan under project No. BR21882439, "Advancement of the Green Energy: Foundational Research of Solar Fuel Technologies for Sustainable Production and Advanced Storage".

Conflict of Interest

The authors declare no conflict of interest.

Abbreviations

DFT – Density functional theory
FCEVs – Fuel-cell electric vehicles
DOE – Department of Energy
MOFs – Metal–organic frameworks
COFs – Covalent organic frameworks
IRMOF– Isoreticular metal–organic frameworks
HKUST-1– Hong Kong University of Science and Technology), which is also called MOF-199
AIMD – Ab initio molecular dynamics
RDG – Reduced density gradient
WDA – Two weighted-density approximations
FMSA – Density expansion method
ADC-substituted MOF-5 – azulenedicarboxylate -

substituted MOF-5
DOS – Density of states analysis
GCMC – Grand canonical Monte Carlo simulation method
DHFUMA – Aliphatic 2,3-dihydroxyfumarate
BDC – Benzenedicarboxylate
DHF – Dihydroxyfumarate
vdW – Van der Waals forces
GR–MOFs – R-graphyne–based MOFs
QTAIM – Quantum Theory of Atoms in Molecules
OMS – Open metal sites
ELF – Electron Localization Function
EDA – Energy decomposition analysis
CT – Charge transfer
BE – Binding energies
ES – Step energies
CBE – Consecutive binding energies
MBFs – Metal–BN frameworks
NDC – Naphthalene dicarboxylate
PBE – Plane-wave basis sets
FTIR – Fourier Transform Infrared Spectroscopy analysis
XRD – X-ray diffraction
SEM–EDX – Scanning electron microscopy coupled with electron-dispersive spectroscopy
Hf-MEL MOF – Hafnium–melamine metal-organic framework
BOMD – Born-Oppenheimer molecular dynamics

Supporting Information

Not applicable.

CRediT Statement

Raushan Soltan: Investigation, Literature review, Writing - Original draft, **Ayaulym Amankeldiyeva:** Literature survey, Writing - Review & editing, **Beksultan Akilbekov:** Literature review analysis, Writing - Review & editing, **Madina Kalibek:** Conceptualization, Writing - Review & editing, **Saniya Sarsenova:** Supervision, Writing - Review & editing; **Zhambul Kerimkulov:** Validation, Writing - Review & editing, **Munziya Abutalip:** Introduction, Writing - Review & Editing, **Yerbolat Magazov:** Formal check, Writing - Review & editing, **Nurlan Almas:** Visualization, Writing - Review & editing, **Nurxat Nuraje:** Supervision, Funding acquisition, Writing - Review & editing, **Mirat Karibayev:** Conceptualization, Supervision, Visualization, Writing - Review & editing.

References

[1] S. Mingolla, P. Gabrielli, A. Manzotti, M. J. Robson, K. Rouwenhorst, F. Ciucci, G. Sansavini, M. M. Klemun, Z. Lu, Effects of emissions caps on the costs and feasibility of low-carbon hydrogen in the European ammonia industry, *Nature Communications*, 2024, **15**, 3753, doi: 10.1038/s41467-024-48145-z.

[2] Y. Magazov, A. Aliyev, K. Moldabekov, A. Rakymbekova, A. Rakymbekova, M. Amze, N. Ibrayev, V. Kudryashov, Photoelectrochemical water splitting using cuprous oxide (Cu_2O)-based photocathode–a review, *ES Energy & Environment*, 2024, **26**, doi: 10.30919/esee1347.

[3] M. K. Kazankapova, B. T. Yermagambet, U. M. Kozhamuratova, Z. T. Dauletzhanova, B. A. Kapsalyamov, A. B. Malgazhdarova, G. K. Mendaliyev, A. Z. Dauletzhanov, N. C. O. Company, Z. M. Kassenova, K. A. Beisembaeva, Obtaining and investigating sorption capacity of carbon nanomaterials derived from coal for hydrogen storage, *ES Energy & Environment*, 2024, **25**, doi: 10.30919/esee1234.

[4] J. A. Turner, Sustainable hydrogen production, *Science*, 2004, **305**, 972-974, doi: 10.1126/science.1103197.

[5] L. Schlapbach, A. Züttel, Hydrogen-storage materials for mobile applications, *Nature*, 2001, **414**, 353-358, doi: 10.1038/35104634.

[6] A. Maiti, J. University, B. Jana, J. University, R. Kumar, J. University, K. Das, J. University, D. Ghoshal, J. University, A chemically robust Zn-MOF with a dual role as a symmetric supercapacitor and sustainable hydrogen storage material, *Inorganic Chemistry*, 2025, **64**, 18332-18345, doi: 10.1021/acs.inorgchem.5c02749.

[7] M. K. Skakov, S. K. Kabdrakhmanova, K. Akatan, A. M. Zhilkashinova, E. Shaimardan, M. M. Beisebekov, K. Nurgamit, V. V. Baklanov, Y. T. Koyanbayev, A. Z. Miniyazov, I. A. Sokolov, N. M. Mukhamedova, La-Cu electrode material for low temperature solid oxide fuel cells, *ES Materials & Manufacturing*, 2023, **22**, doi: 10.30919/esmm969.

[8] W. García-Argote, E. Medel, D. Inostroza, A. Vásquez-Espinal, J. Solar-Encinas, L. Leyva-Parra, L. M. Ruiz, O. Yañez, W. Tiznado, From aromatic motifs to cluster-assembled materials: silicon–lithium nanoclusters for hydrogen storage applications, *Molecules*, 2025, **30**, 2163, doi: 10.3390/molecules30102163.

[9] S. J. Rahaman, A. Samanta, M. H. Mir, B. Dutta, Metal-organic frameworks (MOFs): a promising candidate for stimuli-responsive drug delivery, *ES Materials & Manufacturing*, 2022, **19**, doi: 10.30919/esmm5f792.

[10] V. Mahamiya, A. Shukla, A. K. Adak, H. Lee, N. Seriani, R. Gebauer, Computational simulations and strategies for optimal hydrogen storage materials design, *PRX Energy*, 2025, **4**, 022001, doi: 10.1103/prxenergy.4.022001.

[11] M. K. Dash, S. Giri, I. Chakraborty, S. Bhattacharyya, G. C. De, G. Roymahapatra, Li(0)-pyridine (1: 1) template for efficient hydrogen storage, *ES Materials & Manufacturing*, 2023, **19**, doi: 10.30919/esmm5f825.

[12] R. B. Getman, Y.-S. Bae, C. E. Wilmer, R. Q. Snurr, Review and analysis of molecular simulations of methane, hydrogen, and acetylene storage in metal-organic frameworks, *Chemical Reviews*, 2012, **112**, 703-723, doi: 10.1021/cr200217c.

[13] D. Zhou, C. Zheng, Y. Zhang, H. Sun, P. Sheng, X. Zhang, J. Li, S. Guo, D. Zhao, An overview of RE-Mg-based alloys for hydrogen storage: Structure, properties, progresses and perspectives, *Journal of Magnesium and Alloys*, 2025, **13**, 41-70, doi: 10.1016/j.jma.2024.12.020.

[14] E. H. Akarchaou, R. Touti, A. El Mekkaouy, Y. Didi, A. Tahiri, S. Chtita, Computational analysis of X2MgTiH6 (X =Li, Na, and K) double perovskite hydride materials for hydrogen storage applications, *International Journal of Hydrogen Energy*, 2025, **161**, 150644, doi: 10.1016/j.ijhydene.2025.150644.
[15] S. Nagappan, H. N. Dhandapani, A. Karmakar, S. Kundu, Recent advancement of 2D bi-metallic hydroxides with various strategical modification for the sustainable hydrogen production through water electrolysis, *ES Materials & Manufacturing*, 2023, **19**, doi: 10.30919/esmm5f830.
[16] M. Ali, A. Isah, N. Yekeen, A. Hassanpouryouzband, M. Sarmadivaleh, E. R. Okoroafor, M. Al Kobaisi, M. Mahmoud, V. Vahrenkamp, H. Hoteit, Recent progress in underground hydrogen storage, *Energy & Environmental Science*, 2025, **18**, 5740-5810, doi: 10.1039/D4EE04564E.
[17] Z. Sailau, A. Serikkanov, A. Kemelbekova, A. Shongalova, S. Zhantuarov, N. Almas, A. Aldongarov, K. Toshtay, Insight into the glycerol extraction from biodiesel using deep eutectic solvents, *Journal of Molecular Modeling*, 2023, **29**, 54, doi: 10.1007/s00894-023-05453-3.
[18] S. Nurmanova, S. Kolisnichenko, U. Kokayev, D. Kalmanova, A. Karazhanov, Z. Alipbayev, F. Abuova, O. Abdirashev, B. Satanova, Optimizing waste motor oil recycling into diesel using novel deep eutectic solvents: an atomistic study, *ES Materials & Manufacturing*, 2025, **28**, doi: 10.30919/mm1480.
[19] N. S. Venkataramanan; R. Sahara; H. Mizuseki; Y. Kawazoe, Probing the structure, stability and hydrogen adsorption of lithium functionalized isoreticular MOF-5 (Fe, Cu, Co, Ni and Zn) by density functional theory, *International Journal of Molecular Sciences*, 2009, **10**(4), 1601–1608, doi: 10.3390/ijms10041601.
[20] A. Bag, S. Giri, P. Dhaiveegan, R.T. Jalgham, G. Ch, J. Ganguly, G. Roymahapatra, A theoretical study on Au(I) decorated isomeric triazine complexes as a new class of hydrogen storage materials, *ES Energy and Environment,* 2024, **23**, 1115, doi: 10.30919/esee1115.
[21] T. Duisebayev, M. Abdullah, Y. Tezekbay, M. Zhazitov, N. Kydyrbay, N. Nuraje, O. Toktarbaiuly, Hydrothermal Synthesis and Photocatalytic Performance of Zinc Oxysulfide for Hydrogen Evolution, *Engineered Science,* 2025, **34**, 1460, doi: 10.30919/es1460.
[22] A. Nulimu, A. Aldongarov, S. Sarsenova, A. Ibrayeva, M. Karibayev, Unraveling the Role of Functional Groups in Polyaniline for Ammonia Sensing: A Theoretical Approach, *Engineered Science*, 2025, **36**, 1616, doi:10.30919/es1616.
[23] O. Ismagambetov, N. Aldiyarov, N. Almas, I. Irgibaeva, Z. Baitassova, S. Piskunov, A. Aldongarov, O. Abdirashev, Atomistic modeling of natural gas desulfurization process using task-specific deep eutectic solvents supported by graphene oxide, *Molecules*, 2024, **29**, 5282, doi: 10.3390/molecules29225282.
[24] P. Peng, H. Z. H. Jiang, S. Collins, H. Furukawa, J. R. Long, H. Breunig, Long duration energy storage using hydrogen in metal-organic frameworks: opportunities and challenges, *ACS Energy Letters*, 2024, **9**, 2727-2735, doi: 10.1021/acsenergylett.4c00894.
[25] Y. Basdogan, S. Keskin, Simulation and modelling of MOFs for hydrogen storage, *CrystEngComm*, 2015, **17**, 261-275, doi: 10.1039/c4ce01711k.
[26] R. Li, F. Hu, T. Xia, Y. Li, X. Zhao, J. Zhu, Progress in the application of first principles to hydrogen storage materials, *International Journal of Hydrogen Energy*, 2024, **56**, 1079-1091, doi: 10.1016/j.ijhydene.2023.12.259.
[27] R. A. Alabdulhadi, S. Khan, A. Khan, L. T. Alfuhaid, M. Y. Khan, M. Usman, N. Maity, A. Helal, Potential use of reticular materials (MOFs, ZIFs, and COFs) for hydrogen storage, *ACS Applied Energy Materials*, 2025, **8**, 1397-1413, doi: 10.1021/acsaem.4c02317.
[28] R. B. Getman, Y.-S. Bae, C. E. Wilmer, R. Q. Snurr, Review and analysis of molecular simulations of methane, hydrogen, and acetylene storage in metal-organic frameworks, *Chemical Reviews*, 2012, **112**, 703-723, doi: 10.1021/cr200217c.
[29] A. I. Osman, W. Abd-Elaziem, M. Nasr, M. Farghali, A. K. Rashwan, A. Hamada, Y. M. Wang, M. A. Darwish, T. A. Sebaey, A. Khatab, A. H. Elsheikh, Enhanced hydrogen storage efficiency with sorbents and machine learning: a review, *Environmental Chemistry Letters*, 2024, **22**, 1703-1740, doi: 10.1007/s10311-024-01741-3.
[30] D. Zhao, X. Wang, L. Yue, Y. He, B. Chen, Porous metal–organic frameworks for hydrogen storage, *Chemical Communications*, 2022, **58**, 11059-11078, doi: 10.1039/d2cc04036k.
[31] S. S. Han, J. L. Mendoza-Cortés, W. A. Goddard III, Recent advances on simulation and theory of hydrogen storage in metal–organic frameworks and covalent organic frameworks, *Chemical Society Reviews*, 2009, **38**, 1460-1476, doi: 10.1039/B802430H.
[32] D. Nazarian, J. S. Camp, Y. G. Chung, R. Q. Snurr, D. S. Sholl, Large-scale refinement of metal–organic framework structures using density functional theory, *Chemistry of Materials*, 2017, **29**, 2521-2528, doi: 10.1021/acs.chemmater.6b04226.
[33] X. Yang, Y. Li, Y. Liu, Q. Li, T. Yang, H. Jia, Crystal structure prediction and performance assessment of hydrogen storage materials: insights from computational materials science, *Energies*, 2024, **17**, 3591, doi: 10.3390/en17143591.
[34] M. R. Kalibek, A. D. Ospanova, B. Suleimenova, R. Soltan, T. Orazbek, A. M. Makhmet, K. S. Rafikova, N. Nuraje, Solid-state hydrogen storage materials, *Discover Nano*, 2024, **19**, 195, doi: 10.1186/s11671-024-04137-y.
[35] Y. S. Al-Hamdani, A. Zen, D. Alfè, Unraveling H_2 chemisorption and physisorption on metal decorated graphene using quantum Monte Carlo, *The Journal of Chemical Physics*, 2023, **159**, 204708, doi: 10.1063/5.0174232.
[36] E. Ganz, M. Dornfeld, Energetics and thermodynamics of the initial stages of hydrogen storage by spillover on prototypical metal–organic framework and covalent–organic framework materials, *The Journal of Physical Chemistry C*, 2014, **118**, 5657-5663, doi: 10.1021/jp4105322.
[37] M. EL Kassaoui, M. Loulidi, A. Benyoussef, A. El Kenz, O. Mounkachi, Scandium/lithium-functionalized c-IRMOF-10 as a highly efficient and fast-kinetic hydrogen-storage medium: an *ab*

initio DFT and AIMD study, *ACS Applied Energy Materials*, 2023, **6**, 10897-10907, doi: 10.1021/acsaem.3c01637.
[38] N. Yuksel, A. Kose, M. F. Fellah, A DFT investigation of hydrogen adsorption and storage properties of Mg decorated IRMOF-16 structure, *Colloids and Surfaces A: Physicochemical and Engineering Aspects*, 2022, **641**, 128510, doi: 10.1016/j.colsurfa.2022.128510.
[39] J. Fu, Y. Liu, Y. Tian, J. Wu, Density functional methods for fast screening of metal–organic frameworks for hydrogen storage, *The Journal of Physical Chemistry C*, 2015, **119**, 5374-5385, doi: 10.1021/jp505963m.
[40] S. Yu, S. Li, X. Meng, C. Wan, X. Ju, Tuning the hydrogen adsorption properties of Zn–based metal–organic frameworks: Combined DFT and GCMC simulations, *Journal of Solid State Chemistry*, 2018, **266**, 31-36, doi: 10.1016/j.jssc.2018.04.033.
[41] M. EL Kassaoui, M. Lakhal, A. Benyoussef, A. El Kenz, M. Loulidi, Enhancement of hydrogen storage properties of metal-organic framework-5 by substitution (Zn, Cd and Mg) and decoration (Li, Be and Na), *International Journal of Hydrogen Energy*, 2021, **46**, 26426-26436, doi: 10.1016/j.ijhydene.2021.05.107.
[42] S. Yu, X. Meng, Z. Li, W. Zhang, X. Ju, Heterofullerene C48B12-impregnated MOF-5 and IRMOF-10 for hydrogen storage: a combined DFT and GCMC simulations study, *International Journal of Hydrogen Energy*, 2022, **47**, 39586-39594, doi: 10.1016/j.ijhydene.2022.09.123.
[43] M. EL Kassaoui, M. Lakhal, M. Abdellaoui, A. Benyoussef, A. El Kenz, M. Loulidi, Modeling hydrogen adsorption in the metal organic framework (MOF-5, connector): Z n 4 O (C 8 H_4 O_4) 3, *International Journal of Hydrogen Energy*, 2020, **45**, 33663-33674, doi: 10.1016/j.ijhydene.2020.03.168.
[44] M. EL Kassaoui, M. Lakhal, A. Benyoussef, A. El Kenz, M. Loulidi, Effect of zinc substitution by magnesium and cadmium on hydrogen storage properties of connector-metal-organic framework-5, *Journal of Alloys and Compounds*, 2021, **874**, 159902, doi: 10.1016/j.jallcom.2021.159902.
[45] M. Witman, S. Ling, A. Gladysiak, K. C. Stylianou, B. Smit, B. Slater, M. Haranczyk, Rational design of a low-cost, high-performance metal–organic framework for hydrogen storage and carbon capture, *The Journal of Physical Chemistry C*, 2017, **121**, 1171-1181, doi: 10.1021/acs.jpcc.6b10363.
[46] P. Suksaengrat, V. Amornkitbamrung, P. Srepusharawoot, R. Ahuja, Density functional theory study of hydrogen adsorption in a Ti-decorated Mg-based metal–organic framework-74, *ChemPhysChem*, 2016, **17**, 879-884, doi: 10.1002/cphc.201500981.
[47] T. Nguyen-Thuy, P. Le-Hoang, N. Hoang Vu, T. N. Le, T. Le Hoang Doan, J.-L. Kuo, T. T. Nguyen, T. B. Phan, D. Nguyen-Manh, Hydrogen adsorption mechanism of MOF-74 metal–organic frameworks: an insight from first principles calculations, *RSC Advances*, 2020, **10**, 43940-43949, doi: 10.1039/D0RA08864A.
[48] D. Gygi, E. D. Bloch, J. A. Mason, M. R. Hudson, M. I. Gonzalez, R. L. Siegelman, T. A. Darwish, W. L. Queen, C. M. Brown, J. R. Long, Hydrogen storage in the expanded pore metal–organic frameworks M_2(dobpdc) (M = Mg, Mn, Fe, co, Ni, Zn), *Chemistry of Materials*, 2016, **28**, 1128-1138, doi: 10.1021/acs.chemmater.5b04538.
[49] X. Zhang, Q.-R. Zheng, H.-Z. He, Synergistic effect of hydrogen spillover and nano-confined AlH_3 on room temperature hydrogen storage in MOFs: By GCMC, DFT and experiments, *International Journal of Hydrogen Energy*, 2024, **72**, 1224-1235, doi: 10.1016/j.ijhydene.2023.05.227.
[50] S. Srivastava, S. P. Shet, S. Shanmuga Priya, K. Sudhakar, M. Tahir, Molecular simulation of copper based metal-organic framework (Cu-MOF) for hydrogen adsorption, *International Journal of Hydrogen Energy*, 2022, **47**, 15820-15831, doi: 10.1016/j.ijhydene.2022.03.089.
[51] B. Zhang, Y. Sun, H. Xu, X. He, Hydrogen storage mechanism of metal–organic framework materials based on metal centers and organic ligands, , 2023, **2**, 632-645, doi: 10.1002/cnl2.91.
[52] P. Suksaengrat, V. Amornkitbamrung, P. Srepusharawoot, Enhancements of hydrogen adsorption energy in M-MOF-525 (M= Ti, V, Zr and Hf): a DFT study, *Chinese Journal of Physics*, 2020, **64**, 326-332, doi: 10.1016/j.cjph.2020.01.011.
[53] S. Yu, G. Jing, S. Li, Z. Li, X. Ju, Tuning the hydrogen storage properties of MOF-650: a combined DFT and GCMC simulations study, *International Journal of Hydrogen Energy*, 2020, **45**, 6757-6764, doi: 10.1016/j.ijhydene.2019.12.114.
[54] N. Prasetyo, F. I. Pambudi, Toward hydrogen storage material in fluorinated zirconium metal-organic framework (MOF-801): a periodic density functional theory (DFT) study of fluorination and adsorption, *International Journal of Hydrogen Energy*, 2021, **46**, 4222-4228, doi: 10.1016/j.ijhydene.2020.10.222.
[55] R. Y. Sathe, M. Ussama, H. Bae, H. Lee, T. J. Dhilip Kumar, Density functional theory study of Li-functionalized nanoporous R-graphyne–metal–organic frameworks for reversible hydrogen storage, *ACS Applied Nano Materials*, 2021, **4**, 3949-3957, doi: 10.1021/acsanm.1c00325.
[56] V. M. Vasanthakannan, M. Pavithrakumar, K. Senthilkumar, First principle studies on triphenylene-hexathiol-based metal-organic framework for hydrogen storage application, *Journal of Energy Storage*, 2024, **78**, 110077, doi: 10.1016/j.est.2023.110077.
[57] R. Jose, S. Pal, G. Rajaraman, A theoretical perspective to decipher the origin of high hydrogen storage capacity in Mn(II) metal-organic framework, *ChemPhysChem*, 2023, **24**, e202200257, doi: 10.1002/cphc.202200257.
[58] H. Kwon, D.-E. Jiang, Tuning metal–dihydrogen interaction in metal–organic frameworks for hydrogen storage, *The Journal of Physical Chemistry Letters*, 2022, **13**, 9129-9133, doi: 10.1021/acs.jpclett.2c02628.
[59] A. M. Ahmed Mahmoud, N. Missaoui, S. Nasr, B. Gassoumi, A. Karayel, F. J. Melendez, S. Özkınalı, H. Kahri, H. Kaur, E. A. Lopez Maldonado, M. Mahdouani, R. Bourguiga, C. Sridevi, A. Hosseini-Bandegharaei, H. Barhoumi, Non-surfactant template synthesis of highly porous $Zn_4O(BDC)_3$ and $Cu_3(BTC)_2$ metal–organic frameworks for efficient hydrogen storage: experimental

insights and modeling analysis, *Journal of Energy Storage*, 2025, **123**, 116707, doi: 10.1016/j.est.2025.116707.
[60] G. Xu, Z. Meng, Y. Liu, X. Guo, K. Deng, R. Lu, Heterofullerene-linked metal–organic framework with lithium decoration for storing hydrogen and methane gases, *International Journal of Hydrogen Energy*, 2019, **44**, 6702-6708, doi: 10.1016/j.ijhydene.2019.01.134.
[61] Y. Liu, D. Shen, Z. Tu, L. Xing, Y. G. Chung, S. Li, Room-temperature hydrogen storage performance of metal-organic framework/graphene oxide composites by molecular simulations, *International Journal of Hydrogen Energy*, 2022, **47**, 41055-41068, doi: 10.1016/j.ijhydene.2022.09.199.
[62] K. M. Saidi, B. A. Najri, D. Yıldız, S. Khelili, A. Kivrak, H. Kivrak, Hafnium melamine-based metal-organic frameworks for efficient hydrogen release from sodium borohydride in methanol, *Renewable Energy*, 2026, **256**, 124002, doi: 10.1016/j.renene.2025.124002.
[63] E. Tsivion, S. P. Veccham, M. Head-Gordon, High-temperature hydrogen storage of multiple molecules: theoretical insights from metalated catechols, *Chemphyschem*, 2017, **18**, 184-188, doi: 10.1002/cphc.201601215.
[64] N. T. Xuan Huynh, V. T. Ngan, N. T. Yen Ngoc, V. Chihaia, D. N. Son, Hydrogen storage in M(BDC)(TED)$_{0.5}$ metal–organic framework: physical insights and capacities, *RSC Advances*, 2024, **14**, 19891-19902, doi: 10.1039/D4RA02697G.
[65] M. Asgari, R. Semino, P. Schouwink, I. Kochetygov, O. Trukhina, J. D. Tarver, S. Bulut, S. Yang, C. M. Brown, M. Ceriotti, W. L. Queen, An *In-situ* neutron diffraction and DFT study of hydrogen adsorption in a sodalite-type metal–organic framework, Cu-BTTri, *European Journal of Inorganic Chemistry*, 2019, **2019**, 1147-1154, doi: 10.1002/ejic.201801253.
[66] Z. Ozturk, G. Ozkan, D. Ali Kose, A. Asan, Experimental and simulation study on structural characterization and hydrogen storage of metal organic structured compounds, *International Journal of Hydrogen Energy*, 2016, **41**, 8256-8263, doi: 10.1016/j.ijhydene.2015.11.073.
[67] E. Tsivion, J. R. Long, M. Head-Gordon, Hydrogen physisorption on metal–organic framework linkers and metalated linkers: a computational study of the factors that control binding strength, *Journal of the American Chemical Society*, 2014, **136**, 17827-17835, doi: 10.1021/ja5101323.
[68] G. Nikravesh, E. Salehi, M. Mandooie, A Density Functional Theory (DFT) Investigation on the Impact of the Linker Length in Zinc Oxide-Based Metal-Organic-Frameworks for Hydrogen Adsorption, *Iranian Journal of Chemical Engineering*, 2014, **21**(1), 30–50, doi:10.22034/ijche.2024.419176.1502.
[69] D. E. Jaramillo, H. Z. H. Jiang, H. A. Evans, R. Chakraborty, H. Furukawa, C. M. Brown, M. Head-Gordon, J. R. Long, Ambient-temperature hydrogen storage *via* vanadium(II)-dihydrogen complexation in a metal–organic framework, *Journal of the American Chemical Society*, 2021, **143**, 6248-6256, doi: 10.1021/jacs.1c01883.
[70] S. Kumar, M. Samolia, T. J. Dhilip Kumar, Hydrogen storage in Sc and Li decorated metal–inorganic framework, *ACS Applied Energy Materials*, 2018, **1**, 1328-1336, doi: 10.1021/acsaem.8b00034.
[71] F.-G. Li, C. Liu, D. Yuan, F. Dai, R. Wang, Z. Wang, X. Lu, D. Sun, Ultrahigh hydrogen uptake in an interpenetrated Zn_4O-based metal–organic framework, *CCS Chemistry*, 2022, **4**, 832-837, doi: 10.31635/ccschem.021.202000738.
[72] M. Savage, I. da Silva, M. Johnson, J. H. Carter, R. Newby, M. Suyetin, E. Besley, P. Manuel, S. Rudić, A. N. Fitch, C. Murray, W. I. David, S. Yang, M. Schröder, Observation of binding and rotation of methane and hydrogen within a functional metal-organic framework, *Journal of the American Chemical Society*, 2016, **138**, 9119-9127, doi: 10.1021/jacs.6b01323.
[73] Y. Nanba, T. Tsutsumi, T. Ishimoto, M. Koyama, Theoretical study of the hydrogen absorption mechanism into a palladium nanocube coated with a metal–organic framework, *The Journal of Physical Chemistry C*, 2017, **121**, 14611-14617, doi: 10.1021/acs.jpcc.7b03137.
[74] P. Agarwala, S. K. Pati, L. Roy, Unravelling the possibility of hydrogen storage on naphthalene dicarboxylate-based MOF linkers: a theoretical perspective, *Molecular Physics*, 2020, **118**, e1757169, doi: 10.1080/00268976.2020.1757169.
[75] Z. Meng, X. Yang, Y. Yu, Y. Lyu, Y. Wang, A multiscale simulation approach for enhanced hydrogen storage capacity in hexaazatrinaphthylene-based monolayer metal–organic frameworks, *Chemical Physics Letters*, 2025, **877**, 142264, doi: 10.1016/j.cplett.2025.142264.
[76] A. Kingmaneerat, T. Ratniyomchai, W. Saikong, C. Techawatcharapaikul, T. Kulworawanichpong, Reducing hydrogen consumption by using regenerative braking energy for hydrogen fuel-cell electric bus vehicles, *Engineered Science*, 2024, **33**, doi: 10.30919/es1334.
[77] A. Bag, S. Sinha, H. S. Das, S. Giri, G. C. De, S. Maity, B. B. Xu, Z. Guo, G. Roymahapatra, Hydrogen storage efficiency of the Ag (I)/Au (I) decorated five-member aromatic heterocyclic (AH) compounds: a theoretical investigation, *Engineered Science*, 2023, **28**, doi: 10.30919/es1062.
[78] G. D'Antuono, E. Galloni, D. Lanni, G. Fontana, A relationship for estimating the ignition delay of hydrogen-enriched ammonia-air mixtures, *Engineered Science*, 2023, **28**, doi: 10.30919/es1074.
[79] R. Sawant, S. Chandrakant, S. Kumar, A. Patil, T. Chourushi, Evaluating the thermal performance of methanol and ammonia as working fluids in heat pipes: an experimental and simulation approach, *ES Energy & Environment*, 2025, **28**, doi: 10.30919/ee1484.
[80] A. Seilkhan, A. Kuatbayev, G. Satybaldieva, B. Akbota, S. Zhang, S. Zhang, J. Xu, Z. Idrisheva, Z. Idrisheva, An overview of advancing green energy solutions and environmental protection toward green universities, *ES Energy & Environment*, 2024, **26**, doi: 10.30919/esee1338.
[81] A. U. Abuova, U. Z. Tolegen, T. M. Inerbaev, M. Karibayev, B. M. Satanova, F. U. Abuova, A. I. Popov, A brief review of atomistic studies on $BaTiO_3$ as a photocatalyst for solar water splitting, *Ceramics*, 2025, **8**, 100, doi: 10.3390/ceramics8030100.

[82] N. Kydyrbay, M. Zhazitov, M. Abdullah, T. Duisebayev, Y. Tezekbay, A. Aldongarov, M. Karibayev, N. Nuraje, O. Toktarbaiuly, Structural, surface, and theoretical investigation of hydrophobic-modified nanodiamond powders, *Scientific Reports*, 2025, **15**, 24329, doi: 10.1038/s41598-025-10027-9.
[83] B. Myrzakhmetov, A. Akhmetova, A. Bissenbay, M. Karibayev, X. Pan, Y. Wang, Z. Bakenov, A. Mentbayeva, Review: chitosan-based biopolymers for anion-exchange membrane fuel cell application, *Royal Society Open Science*, 2023, **10**, 230843, doi: 10.1098/rsos.230843.
[84] M. Karibayev, B. Myrzakhmetov, D. Bekeshov, Y. Wang, A. Mentbayeva, Atomistic modeling of quaternized chitosan head groups: insights into chemical stability and ion transport for anion exchange membrane applications, *Molecules*, 2024, **29**, 3175, doi: 10.3390/molecules29133175.
[85] F. Zeraatkar-Kashani, M. Mohsennia, R. Foulady-Dehaghi, Evaluation of hydrogen storage capacity of the synthesized amino-functionalized Cu-based MOF/COF hybrid material, *Journal of Energy Storage*, 2025, **122**, 116664, doi: 10.1016/j.est.2025.116664.
[86] Y. Chen, B. Sun, G. Zhang, S. Ni, C. Li, J. Tian, Y. Zhang, X. Li, MOF-derived $Ni_3Fe/Ni/NiFe_2O_4$@C for enhanced hydrogen storage performance of MgH_2, *Journal of Energy Chemistry*, 2025, **101**, 333-344, doi: 10.1016/j.jechem.2024.09.048.
[87] Z. Yang, Y. Wang, X. Lin, Y. Zou, C. Xiang, F. Xu, L. Sun, Y. S. Chua, Vanadium induces Ni-Co MOF formation from a NiCo LDH to catalytically enhance the MgH_2 hydrogen storage performance, *Journal of Magnesium and Alloys*, 2025, **13**, 4020-4031, doi: 10.1016/j.jma.2025.01.012.
[88] J. Steffen, Simulation of hydrogen storage in MOF-5 and Li-MOF-5 by ring polymer molecular dynamics on self-consistently fine-tuned machine-learned interatomic potentials, *The Journal of Physical Chemistry C*, 2025, **129**, 13513-13531, doi: 10.1021/acs.jpcc.5c01522.
[89] K. Yang, Z. Zhang, X. Zhang, Q. Wang, X. Hao, G. Ye, J. Luo, H. Yang, Energy performance evaluation and life cycle assessment on a novel hydrogen storage system with cryo-adsorption approach using MOF, *Chemical Engineering Journal*, 2025, **520**, 165656, doi: 10.1016/j.cej.2025.165656.
[90] J.-Q. Hu, W. Jiang, N. Si, Z. Wang, Z. Cao, Synergistic effect of MOF-derived carbon-supported CoNi and FeNi bimetallic catalysts on hydrogen storage kinetics of MgH_2, *Journal of Energy Storage*, 2025, **123**, 116824, doi: 10.1016/j.est.2025.116824.
[91] M. C. Tapia, B. G. Alamani, T.-H. Bae, Enhancing hydrogen storage in MOF/graphene composites: The impact of graphene oxide and porous graphene oxide on adsorptive performance, *Separation and Purification Technology*, 2025, **363**, 132313, doi: 10.1016/j.seppur.2025.132313.
[92] K. Liu, H. Chen, T. Islamoglu, A. S. Rosen, X. Wang, O. K. Farha, R. Q. Snurr, Computational investigation of the impact of metal–organic framework topology on hydrogen storage capacity, *Molecular Systems Design & Engineering*, 2025, **10**, 817-835, doi: 10.1039/d5me00078e.
[93] Y. Zhang, Y. Zhang, T. Hu, A porous three-dimensional Cu-MOF: preparation and application in supercapacitors, low temperature hydrogen storage and gas separation, *Inorganica Chimica Acta*, 2025, **575**, 122414, doi: 10.1016/j.ica.2024.122414.
[94] W.-T. Kim, W.-G. Lee, H.-E. An, H. Furukawa, W. Jeong, S.-C. Kim, J. R. Long, S. Jeong, J.-H. Lee, Machine learning-assisted design of metal–organic frameworks for hydrogen storage: a high-throughput screening and experimental approach, *Chemical Engineering Journal*, 2025, **507**, 160766, doi: 10.1016/j.cej.2025.160766.
[95] L. Jimenez-Lopez, R. Morales Ospino, L. G. de Araujo, A. Celzard, V. Fierro, Latest developments in the synthesis of metal–organic frameworks and their hybrids for hydrogen storage, *Nanoscale*, 2025, **17**, 6390-6413, doi: 10.1039/d4nr03969f.
[96] S. Xi, L. Gao, W. Yao, J. Huang, R. Chen, W. Wu, D. Xu, X. Dong, H. Wang, M. Gong, T. Zhang, B. Wang, Study on the low-temperature and high-pressure hydrogen storage performance of MIL-101(Cr)-filled type III tank, *International Journal of Hydrogen Energy*, 2025, **128**, 95-104, doi: 10.1016/j.ijhydene.2025.04.219.
[97] M. Zhazitov, M. Abdullah, N. Kydyrbay, E. Adotey, Z. Toktarbay, T. Duisebayev, Y. Tezekbay, N. Nuraje, O. Toktarbaiuly, Fabrication of mechanically resistant ZnO-based superhydrophobic material for enhanced concrete applications, *Case Studies in Construction Materials*, 2025, **22**, e04655, doi: 10.1016/j.cscm.2025.e04655.
[98] G. Provinciali, N. A. Consoli, R. Caliandro, V. Mangini, L. Barba, C. Giannini, G. Tuci, G. Giambastiani, M. Lelli, A. Rossin, Ammonia borane and hydrazine bis(borane) confined within zirconium bithiazole and bipyridyl metal–organic frameworks as chemical hydrogen storage materials, *The Journal of Physical Chemistry C*, 2025, **129**, 6094-6108, doi: 10.1021/acs.jpcc.5c00187.
[99] G. Yang, J. Lv, Q. Yang, Q. Wang, Full-spectrum photocatalytic hydrogen production by MOFs materials-a minireview, *Materials Today Sustainability*, 2025, **31**, 101186, doi: 10.1016/j.mtsust.2025.101186.
[100] T. Pisarenko, N. Papež, M. A. Al-Anber, R. Dallaev, K. Částková, Ş. Ţălu, A development and comparison study of PVDF membranes enriched by metal-organic frameworks, *Polymers*, 2025, **17**, 1140, doi: 10.3390/polym17091140.
[101] Y. Tezekbay, T. Duisebayev, Z. Taubaldiyeva, A. Abduvalov, N. Nuraje, O. Toktarbaiuly, Photocatalytic optimization of ZnO–Ga_2O_3 composite thin films for PEC water splitting: effects of thickness, environment, and annealing temperature, *RSC Advances*, 2025, **15**, 27586-27593, doi: 10.1039/D5RA03463A.
[102] X. Huang, Y. Cui, N. Kumar, J. Sun, Y. Lin, N. Nuraje, C. Wang, Advances in hydrogel-based solar-driven interfacial evaporation systems: The pivotal factors and design strategies from photothermal engineering to energy management, *Separation and Purification Technology*, 2025, **379**, 134834, doi: 10.1016/j.seppur.2025.134834.
[103] M. Karibayev, D. Bekeshov, B. Myrzakhmetov, S. Kalybekkyzy, Y. Wang, Z. Bakenov, A. Mentbayeva, Effect of

hydration on the intermolecular interaction of various quaternary ammonium based head groups with hydroxide ion of anion exchange membrane studied at the molecular level, *Eurasian Chemico-Technological Journal*, 2023, **25**, 89, doi: 10.18321/ectj1499.

Publisher's Note: Engineered Science Publisher remains neutral with regard to jurisdictional claims in published maps and institutional affiliations.